

# An alternative paradigm of fault diagnosis in dynamic systems: orthogonal projection-based methods

Steven X. Ding<sup>1</sup>, Linlin Li<sup>2</sup>, and Tianyu Liu<sup>1</sup>

<sup>1</sup>Institute for Automatic Control and Complex Systems, University of Duisburg-Essen, 47057, Duisburg, Germany

<sup>2</sup>School of Automation and Electrical Engineering, University of Science and Technology Beijing, Beijing 100083, P. R. China (Corresponding author)

**Abstract:** In this paper, we propose a new paradigm of fault diagnosis in dynamic systems as an alternative to the well-established observer-based framework. The basic idea behind this work is to (i) formulate fault detection and isolation as projection of measurement signals onto (system) subspaces in Hilbert space, and (ii) solve the resulting problems by means of projection methods with orthogonal projection operators and gap metric as major tools. In the new framework, fault diagnosis issues are uniformly addressed both in the model-based and data-driven fashions. Moreover, the design and implementation of the projection-based fault diagnosis systems, from residual generation to threshold setting, can be unifiedly handled. Thanks to the well-defined distance metric for projections in Hilbert subspaces, the projection-based fault diagnosis systems deliver optimal fault detectability. In particular, a new type of residual-driven thresholds is proposed, which significantly increases the fault detectability. In this work, various design schemes are proposed, including a basic projection-based fault detection scheme, fault detection schemes for feedback control systems, fault classification as well as two modified fault detection schemes. As a part of our study, relations to the existing observer-based fault detection systems are investigated, which showcases that, with comparable online computations, the proposed projection-based detection methods offer improved detection performance.

**Keywords:** Fault detection and classification, orthogonal projection, operators, gap metric, observer-based fault detection, parametric and multiplicative faults.

## 1 Introduction

Observer-based fault diagnosis is the state of the art technique in dealing with fault detection, isolation and identification in dynamic systems (Patton *et al.*, 1989; Gertler, 1998; Chen and Patton, 1999; Blanke *et al.*, 2006; Ding, 2008). Beginning 50 years ago with the pioneer work (Beard, 1971; Jones, 1973), observer-based fault diagnosis technique has undergone a rapid development over a couple of decades and become today well established as an active research area in control theory and engineering (Frank, 1990; Frank and Ding, 1997;

Venkatasubramanian *et al.*, 2003; Mangoubi *et al.*, 2009; Hwang *et al.*, 2010; Gao *et al.*, 2015; Zhong *et al.*, 2018). Even in the era that data-driven and machine learning methods become the most dominant research domain in technical fault diagnosis, observer-based fault diagnosis technique is still the major and efficient tool applied to addressing fault diagnosis issues for dynamic and particularly automatic control systems (Ding, 2020). The recent development of data-driven design of observer-based fault detection systems (Ding, 2014a; Ding, 2014b) has extended the application of this technique to meet practical demands.

An observer-based fault diagnosis system consists of two major functional blocks: residual (feature) generation and decision making. While decisions for fault detection or isolation are made on the basis of residual processing algorithms, the major task of residual generation is the construction of an observer serving as residual generator. Thanks to this intimate relation to control theory, most of investigations on observer-based fault diagnosis systems are dedicated to observer design issues. Keeping in mind that any fault detection (or isolation) problem is in its core to distinguish two different system operations, i.e. the fault (to be detected) vs. uncertainties as fault detection, or two different classes of faults as fault isolation, research on observer-based residual generation, beginning in its early stage, was shaped into the trade-off framework of sensitivity (e.g. to fault) vs. robustness (against uncertainty) (Frank, 1990; Ding *et al.*, 1993; Patton and Chen, 1993; Frank and Ding, 1994; Hou and Patton, 1996). This development is a natural result, as robust control dominated control theory and engineering between 80's and 90's, and has stamped the progress of observer-based fault diagnosis technique since then. Reviewing the literature in the relevant research and application domains gives the impression that there is no more efficient and systematic alternative to observer-based fault diagnosis technique in dealing with fault diagnosis in dynamic systems, although there exist a number of open and challenging issues even after extensive studies over past decades. These include,

- efficient and optimal detection of parametric (multiplicative) faults, in particular in the presence of model uncertainties as well as in feedback control systems,
- definition and introduction of convincing and mathematically well-established metrics to measure the distance between nominal and faulty operations for fault detection purpose or the distance between two different classes of faults towards fault isolation. Although the widely accepted optimisation criteria like  $\mathcal{H}_\infty/\mathcal{H}_\infty$ ,  $\mathcal{H}_-/\mathcal{H}_\infty$  and  $\mathcal{H}_2$  (Ding *et al.*, 1993; Frank and Ding, 1994; Hou and Patton, 1996; Ding *et al.*, 2000; Zhong *et al.*, 2003; Wang *et al.*, 2007) are applied for optimal design of observer-based residual generators, they only reflect the influences of faults and uncertainties on system dynamics under consideration, and are not metric for measuring the distance of different system operations,
- residual generation and threshold setting in an integrated manner. This is indeed the consequence of the above-mentioned problem with missing metric for distance measurement, and
- a uniform design of fault diagnosis systems, both in the model-based and data-driven fashions.

These facts have considerably motivated us to explore potential alternative strategies in recent years.

Hilbert space  $\mathcal{H}$  is a vector space endowed with an inner product  $\langle \cdot, \cdot \rangle$ . Given a vector  $\alpha \in \mathcal{H}$ , the norm of  $\alpha$  is induced by the inner product,  $\|\alpha\|^2 = \langle \alpha, \alpha \rangle$ . In this regard, Hilbert space is a complete metric space (Kato, 1995; Feintuch, 1998). Accordingly, a classification problem can be well defined in Hilbert space as: given a subspace  $\mathcal{K} \in \mathcal{H}$ , check if  $\alpha \in \mathcal{K}$ . The solution is straightforward and consists of two steps: (i) projecting  $\alpha$  onto  $\mathcal{K}$ , and then (ii) calculating the distance between  $\alpha$  and its projection using the induced norm. Figure 1 schematically illustrates this projection-based classification problem and its solution.

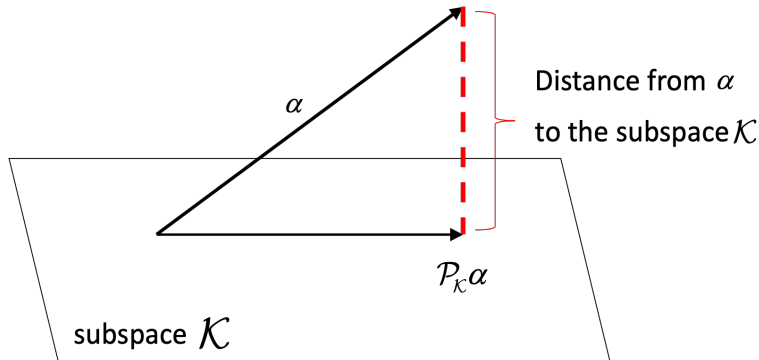


Figure 1: Schematic description of projection-based classification ( $\mathcal{P}_{\mathcal{K}}\alpha$  denotes the projection of  $\alpha$  onto  $\mathcal{K}$ )

This conceptual formulation of classification problem in terms of projection and distance in Hilbert subspace, and above all, the facts that

- all signals in dynamic system can be represented by vectors in a Hilbert subspace (Francis, 1987), and
- system dynamics can be modelled as subspaces in Hilbert space as well (Francis, 1987; Vinnicombe, 2000; Feintuch, 1998)

are convincing arguments for us to study fault diagnosis issues using projection-based methods in the above described context. To this end, we will first formulate fault detection and isolation issues, in particular those open ones like detecting parametric faults in uncertainty systems or fault detection in feedback control systems, as classification problems in Hilbert subspaces and solve them using projection-based methods. This is the *first* (intended) *contribution* of our work towards establishing an alternative paradigm for fault diagnosis in dynamic systems. We will further demonstrate that, in this framework, fault detection and isolation issues can be systematically handled in a uniform manner. To be specific, residual generation and threshold setting will be addressed by determining (i) the distance of a (signal) vector to a (system) subspace and (ii) the gap between two (system) subspaces. In particular, the threshold becomes residual-driven, which significantly increases the fault detectability. These results would be the *second contribution* of our work. In our study, considerable attention will be paid to relations between the proposed projection-based methods and the well-established observer-based framework as well, and comparison will be made when possible. As the *third contribution*, it will be demonstrated that the proposed projection-based methods result in higher fault detectability. Moreover, a projection-based fault detection system will be proposed, which is comparable with the existing observer-based

systems with regard to the needed online computation, but delivers better fault detection performance.

Projection methods are a standard technique in machine and statistic learning and extensively applied in data-driven fault diagnosis. The most popular ones are principal component analysis (PCA) method (Jolliffe, 1986; Chiang *et al.*, 2001; Qin, 2003; Ding, 2014*a*) and partial least squares (PLS) algorithm (Chiang *et al.*, 2001; Li *et al.*, 2010; Ding, 2014*a*). Although their application is limited to detecting faults in statistic processes (including steady dynamic systems), PCA and PLS are, thanks to their uniform formulation and computations, and above all, their clear geometric interpretation of projection onto subspaces, not only widely accepted in industry, but also recognised in research as a conceptional basis for the development of advanced fault diagnosis methods. This example also inspires our efforts towards a projection-based fault diagnosis framework. Noticing that projections adopted in PCA and PLS deal with linear algebraic computations, and thus are limited to solving fault diagnosis problems in statistic processes, different mathematical and control theoretic tools are needed for our study on fault diagnosis in dynamic systems. We will consider system signals (data) defined in Hilbert spaces like Lebesgue space or Hardy space, and model the dynamic systems under consideration as subspaces in Hilbert space, for instance, image and kernel subspaces (Francis, 1987; Vinnicombe, 2000). In order to deal with orthogonal projections and distance between (signal) vector and (system) subspace or gap between two subspaces, basics of operator theory, gap metric as well as their computations and realisations in form of dynamic systems will serve as the major tools for our study.

The paper is organised as follows. In Section 2, necessary preliminaries of system representations, orthogonal projection in Hilbert space as well as gap metric as a similarity measurement between two Hilbert subspaces are introduced. Section 3 is dedicated to the establishment of the basic form of the projection-based fault detection framework. It includes (i) formulation and solution of orthogonal projection-based residual generation, (ii) the realisation and online computation algorithms, and (iii) gap metric-based threshold setting. Section 4 demonstrates solutions of fault detection in feedback control systems achieved in the framework of projection-based fault detection. In Section 5, fault detection and isolation issues are formulated as binary and multi-class classification problems and solved by means of projection-based methods. Two modified projection-based fault detection methods are proposed in Section 6. The first one is comparable with existing observer-based fault detection schemes with regard to the associated online computation. The second one provides us with a practical solution with finite evaluation time interval. This method can be realised in the data-driven fashion as well. In our experimental study in Section 7, applications of some of the proposed methods and algorithms are illustrated on a laboratory three-tank system. Finally, in Section 8, the major results are first summarised, and two remarks on (i) the projection-based interpretation of the so-called unified solution for detecting additive faults, and (ii) computation of a type of gap metric are included.

Throughout this paper, standard notations known in advanced control theory and linear algebra are adopted. In addition,  $\mathcal{L}_2(-\infty, \infty) = \mathcal{L}_2(-\infty, 0] \oplus \mathcal{L}_2[0, \infty)$  is time domain space of all square summable Lebesgue signals (signals with bounded energy).  $\mathcal{H}_2$  is the space of Fourier transforms of signals in  $\mathcal{L}_2[0, \infty)$ .  $\mathcal{H}_\infty$  ( $\mathcal{RH}_\infty$ ) is used to denote the set of all stable systems (with a real rational transfer function). For transfer matrix  $G(z)$ ,  $G^\sim(z) = G^T(z^{-1})$ . By the application of projection-based methods, following notations are adopted.  $\mathcal{P}_{\mathcal{I}}$  denotes

an orthogonal projection onto subspace  $\mathcal{I}$ , which is an operator whose norm is denoted by  $\|\mathcal{P}_{\mathcal{I}}\|$ .  $\mathcal{P}_{\mathcal{I}}^*$  is the adjoint of  $\mathcal{P}_{\mathcal{I}}$ .  $\mathcal{K}^\perp$  represents the orthogonal complement of  $\mathcal{K}$ .  $\mathcal{L}_K$  stands for Laurent (multiplication) operator with symbol  $K$  (Francis, 1987; Vinnicombe, 2000; Feintuch, 1998).

## 2 Preliminaries

As the methodological basis of our work, we first introduce the concepts of kernel and image representations as alternative system model forms and some associated computation issues. It is followed by the introduction of orthogonal projection in Hilbert space and gap metric as a similarity measurement between two closed Hilbert subspaces.

### 2.1 Kernel and image representations and subspaces

Consider discrete-time linear time invariant (LTI) systems modelled by

$$y(z) = G(z)u(z), y(z) \in \mathbb{C}^m, u(z) \in \mathbb{C}^p \quad (1)$$

with  $u$  and  $y$  as the plant input and output vectors. It is assumed that  $G(z)$  is a proper real-rational matrix and its minimal state space realisation is given by

$$x(k+1) = Ax(k) + Bu(k), x(0) = x_0, \quad (2)$$

$$y(k) = Cx(k) + Du(k), \quad (3)$$

where  $x \in \mathbb{R}^n$  is the state vector and  $x_0$  is the initial condition of the system. Matrices  $A, B, C, D$  are appropriately dimensioned real constant matrices. A factorisation of a transfer function matrix over  $\mathcal{RH}_\infty$  gives a further system representation form and factorises the transfer matrix into two stable transfer matrices. The left and right factorisations (LF and RF) of  $G(z)$  are given by

$$G(z) = \hat{M}^{-1}(z)\hat{N}(z) = N(z)M^{-1}(z), \quad (4)$$

whose state space representations are

$$\hat{M}(z) = (A - LC, -L, WC, W), \hat{N}(z) = (A - LC, B - LD, WC, WD), \quad (5)$$

$$M(z) = (A + BF, BV, F, V), N(z) = (A + BF, BV, C + DF, DV), \quad (6)$$

where (real) matrices  $F$  and  $L$  are selected such that  $A + BF$  and  $A - LC$  are Schur matrices, and  $W$  and  $V$  are invertible (Hoffmann, 1996).  $(\hat{M}, \hat{N})$  and  $(M, N)$  build left and right coprime pairs (LCP and RCP), if there exist  $(\hat{X}, \hat{Y})$  and  $(X, Y)$  over  $\mathcal{RH}_\infty$  so that the Bezout identity holds

$$\begin{bmatrix} X(z) & Y(z) \\ -\hat{N}(z) & \hat{M}(z) \end{bmatrix} \begin{bmatrix} M(z) & -\hat{Y}(z) \\ N(z) & \hat{X}(z) \end{bmatrix} = \begin{bmatrix} I & 0 \\ 0 & I \end{bmatrix}. \quad (7)$$

The state space computation formulas of  $(\hat{X}, \hat{Y})$  and  $(X, Y)$  are (Hoffmann, 1996)

$$\hat{X}(z) = (A + BF, L, C + DF, W^{-1}), \hat{Y}(z) = (A + BF, -LW^{-1}, F, 0), \quad (8)$$

$$X(z) = (A - LC, -(B - LD), F, V^{-1}), Y(z) = (A - LC, -L, V^{-1}F, 0). \quad (9)$$

It follows from (4)-(6) that

- the LCP of  $G(z)$  can be equivalently written as

$$r_0(z) = \hat{M}(z)y(z) - \hat{N}(z)u(z) \implies \quad (10)$$

$$\hat{x}(k+1) = (A - LC)\hat{x}(k) + (B - LD)u(k) + Ly(k), \quad (11)$$

$$r_0(k) = W(y(k) - \hat{y}(k)), \hat{y}(k) = C\hat{x}(k) + Du(k), \quad (12)$$

and, if  $x(0) = \hat{x}(0)$ , it holds  $r_0(k) = 0$ ,

- the RCP of  $G(z)$  can be represented by, for some  $v \in \mathcal{H}_2$ ,

$$u(z) = M(z)v(z) \iff M^{-1}(z)u(z) = v(z), y(z) = N(z)v(z) \implies \quad (13)$$

$$x(k+1) = (A + BF)x(k) + BVv(k) \quad (14)$$

$$\begin{bmatrix} u(k) \\ y(k) \end{bmatrix} = \begin{bmatrix} F \\ C + DF \end{bmatrix} x(k) + \begin{bmatrix} V \\ DV \end{bmatrix} v(k). \quad (15)$$

System (10)-(12) is the well-known observer-based residual generator with  $r_0(k)$  being a residual vector and  $W$  as a post-filter, while system (13)-(15) describes the closed-loop dynamics of a state feedback control with  $v(k)$  as reference vector and  $V$  as a pre-filter. Systems (10)-(12) and (13)-(15) are called stable kernel and image representations (SKR and SIR) of  $G(z)$ . For the sake of simplicity, we introduce the following notation for SKR and SIR,

$$\text{SKR} : r_0(z) = \begin{bmatrix} -\hat{N}(z) & \hat{M}(z) \end{bmatrix} \begin{bmatrix} u(z) \\ y(z) \end{bmatrix}, \quad (16)$$

$$\text{SIR} : \begin{bmatrix} u(z) \\ y(z) \end{bmatrix} = \begin{bmatrix} M(z) \\ N(z) \end{bmatrix} v(z). \quad (17)$$

In our subsequent study, the so-called normalised SKR and SIR play an important role, which are denoted by  $K_G$  and  $I_G$  and defined by

$$\begin{aligned} K_G(z)K_G^\sim(z) &= \hat{N}_0(z)\hat{N}_0^\sim(z) + \hat{M}_0(z)\hat{M}_0^\sim(z) = I, \\ I_G^\sim(z)I_G(z) &= M_0^\sim(z)M_0(z) + N_0^\sim(z)N_0(z) = I, \end{aligned}$$

where  $(\hat{M}_0, \hat{N}_0)$  and  $(M_0, N_0)$  are LCP and RCP with  $L = L_0, W = W_0, F = F_0$  and  $V = V_0$ , as given below (Hoffmann, 1996):

$$L = L_0 = (BD^T + APC^T)(I + DD^T + CPC^T)^{-1}, \quad (18)$$

$$W = W_0 = U(I + DD^T + CPC^T)^{-1/2}, UU^T = I \iff W_0(I + DD^T + CPC^T)W_0^T = I, \quad (19)$$

$$F = F_0 = -(I + D^T D + B^T QB)^{-1}(D^T C + B^T QA), \quad (20)$$

$$V = V_0 = (I + D^T D + B^T QB)^{-1/2} \Gamma, \Gamma^T \Gamma = I \iff V_0^T (I + D^T D + B^T QB) V_0 = I. \quad (21)$$

Here,  $P > 0, Q > 0$  solve the following Riccati equations respectively,

$$\begin{aligned} P &= APA^T + BB^T - (BD^T + APC^T)(I + DD^T + CPC^T)^{-1}(BD^T + APC^T)^T, \\ Q &= A^T QA + C^T C - (D^T C + B^T QA)^T (I + D^T D + B^T QB)^{-1}(D^T C + B^T QA). \end{aligned}$$

**Remark 1** Hereafter, we may drop out the domain variable  $z$  or  $k$  when there is no risk of confusion.

The  $\mathcal{H}_2$  input and output vectors  $\begin{bmatrix} u \\ y \end{bmatrix}$  satisfying (10)-(12) or generated by  $v \in \mathcal{H}_2$  according to (13)-(15) build subspaces in  $\mathcal{H}_2$ . For our purpose, the following definitions of kernel and image subspaces are introduced.

**Definition 1** Given the model (1) and the corresponding LCP and RCP  $(\hat{M}, \hat{N})$  and  $(M, N)$ , the  $\mathcal{H}_2$  subspace  $\mathcal{K}_G$  defined by

$$\mathcal{K}_G = \left\{ \begin{bmatrix} u \\ y \end{bmatrix} \in \mathcal{H}_2 : \begin{bmatrix} -\hat{N} & \hat{M} \end{bmatrix} \begin{bmatrix} u \\ y \end{bmatrix} = 0 \right\} \quad (22)$$

is called kernel subspace of  $G$ , and the  $\mathcal{H}_2$  subspace  $\mathcal{I}_G$  defined by

$$\mathcal{I}_G = \left\{ \begin{bmatrix} u \\ y \end{bmatrix} \in \mathcal{H}_2 : \begin{bmatrix} u \\ y \end{bmatrix} = \begin{bmatrix} M \\ N \end{bmatrix} v, v \in \mathcal{H}_2 \right\} \quad (23)$$

is image subspace.

It is evident that the kernel and image subspaces  $\mathcal{K}_G$  and  $\mathcal{I}_G$  consist of all (bounded) input and output pairs  $(u, y)$ . They are closed subspace in  $\mathcal{H}_2$  (Vinnicombe, 2000).

## 2.2 Orthogonal projection and gap metric

An orthogonal projection on a subspace  $\mathcal{V}$ , denoted by  $\mathcal{P}_{\mathcal{V}}$ , in Hilbert space endowed with the inner product,

$$\langle x, y \rangle = \sum_{k=0}^{\infty} x^T(k)y(k), x, y \in \mathcal{H}_2, \quad (24)$$

is a linear operator satisfying (Kato, 1995)

$$x, y \in \mathcal{V}, \mathcal{P}_{\mathcal{V}}^2 = \mathcal{P}_{\mathcal{V}}, \langle \mathcal{P}_{\mathcal{V}}x, y \rangle = \langle x, \mathcal{P}_{\mathcal{V}}y \rangle. \quad (25)$$

The following well-known properties of an orthogonal projection are of importance for our subsequent study (Kato, 1995; Feintuch, 1998):

- given  $x \in \mathcal{H}_2$ , the (orthogonal) projection of  $x$  onto  $\mathcal{V}$ ,  $\mathcal{P}_{\mathcal{V}}x$ , satisfies

$$\langle \mathcal{P}_{\mathcal{V}}x, x - \mathcal{P}_{\mathcal{V}}x \rangle = 0. \quad (26)$$

Often,  $\mathcal{P}_{\mathcal{V}}x$  serves as an estimate for  $x$ , and in this context,  $x - \mathcal{P}_{\mathcal{V}}x$  is understood as the estimation error. That means, the projection-induced estimate is orthogonal to the estimation error;

- relation (26) can also be equivalently expressed by

$$x = \mathcal{P}_{\mathcal{V}}x + \mathcal{P}_{\mathcal{V}^\perp}x,$$

where  $\mathcal{V}^\perp$  is the orthogonal complement of  $\mathcal{V}$ ;

- and given  $y \in \mathcal{H}_2, \forall x \in \mathcal{V} \in \mathcal{H}_2$ ,

$$\langle y - x, y - x \rangle = \|y - x\|_2^2 \geq \|y - \mathcal{P}_{\mathcal{V}}y\|_2^2. \quad (27)$$

Given a closed subspace  $\mathcal{V} \in \mathcal{H}_2$  and a vector  $y \in \mathcal{H}_2$ , the distance between  $y$  and  $\mathcal{V}$ ,  $dist(y, \mathcal{V})$ , is defined as

$$dist(y, \mathcal{V}) = \inf_{x \in \mathcal{V}} \|y - x\|_2,$$

which, following (27), can be computed as

$$dist(y, \mathcal{V}) = (\mathcal{I} - \mathcal{P}_{\mathcal{V}})y = \mathcal{P}_{\mathcal{V}^\perp}y.$$

Here,  $\mathcal{I}$  is the unit operator.

In order to measure the similarity of two (closed) subspaces in Hilbert space  $\mathcal{H}$ , the concept of gap metric is established (Kato, 1995; Feintuch, 1998). Given two closed subspaces  $\mathcal{V}, \mathcal{U} \in \mathcal{H}$ , the gap metric between them is defined by

$$\delta(\mathcal{V}, \mathcal{U}) = \max \left\{ \vec{\delta}(\mathcal{V}, \mathcal{U}), \vec{\delta}(\mathcal{U}, \mathcal{V}) \right\}, \quad (28)$$

$$\vec{\delta}(\mathcal{V}, \mathcal{U}) = \sup_{\substack{x \in \mathcal{V} \\ \|x\|_2=1}} dist(x, \mathcal{U}) = \|(\mathcal{I} - \mathcal{P}_{\mathcal{U}})\mathcal{P}_{\mathcal{V}}\| = \sup_{x \in \mathcal{V}} \inf_{y \in \mathcal{U}} \frac{\|x - y\|_2}{\|x\|_2}, \quad (29)$$

$$\vec{\delta}(\mathcal{U}, \mathcal{V}) = \sup_{\substack{y \in \mathcal{U} \\ \|y\|_2=1}} dist(y, \mathcal{V}) = \|(\mathcal{I} - \mathcal{P}_{\mathcal{V}})\mathcal{P}_{\mathcal{U}}\| = \sup_{y \in \mathcal{U}} \inf_{x \in \mathcal{V}} \frac{\|y - x\|_2}{\|y\|_2}. \quad (30)$$

Here,  $\vec{\delta}(\mathcal{V}, \mathcal{U})$  and  $\vec{\delta}(\mathcal{U}, \mathcal{V})$  are called directed gap. The following properties are well-known (Kato, 1995; Feintuch, 1998) and useful for our subsequent investigation:

$$\begin{aligned} 0 &\leq \delta(\mathcal{V}, \mathcal{U}) \leq 1, \\ \text{for } \delta(\mathcal{V}, \mathcal{U}) < 1, &\vec{\delta}(\mathcal{V}, \mathcal{U}) = \vec{\delta}(\mathcal{U}, \mathcal{V}) = \delta(\mathcal{V}, \mathcal{U}), \\ \text{for } \delta(\mathcal{V}, \mathcal{U}) = 0, &\mathcal{V} = \mathcal{U}, \text{ and } \delta(\mathcal{V}, \mathcal{U}) = 1, \mathcal{V} \perp \mathcal{U}. \end{aligned}$$

## 2.3 Problem formulation

With the aid of the defined image/kernel subspace and orthogonal projection operator, we are now in the position to concretise fault detection problem in terms of projection-based classification, as sketched in Figure 1. Given system measurement vector  $\begin{bmatrix} u \\ y \end{bmatrix} \in \mathcal{H}_2$ , find its orthogonal projection onto image subspace  $\mathcal{I}_G, \mathcal{P}_{\mathcal{I}_G}$ , and further determine the distance  $dist\left(\begin{bmatrix} u \\ y \end{bmatrix}, \mathcal{I}_G\right)$  so that a decision can be made on the basis of the distance value with respect to an established threshold. In this regard, the following problems should be solved at first:

- definition of orthogonal projection operator and computation of  $dist\left(\begin{bmatrix} u \\ y \end{bmatrix}, \mathcal{I}_G\right)$ ,
- online realisation algorithm towards constructing a fault detection system, and



- determination of threshold. In our work, threshold is to be set to guarantee that model uncertainties will not cause false alarms.

This work is essential to establish the intended projection-based fault diagnosis framework. The first application in this framework is detecting (parametric) faults in feedback control systems, a challenging and open issue. As further topics, we will study fault detection and isolation, formulated as binary and multi-class classification problems, in the projection-based framework.

In our work, attention will be paid to comparison study with the well-established observer-based fault diagnosis methods when possible. In this context, we will propose a modified projection-based fault detection scheme that is comparable with an observer-based fault detection system with regard to online computation but delivers better detection performance. Considering that realisation of the inner product defined in (24) requires, theoretically, data over  $[0, \infty)$ , a further modified projection-based method will be developed, which allows an optimal fault detection over finite time interval. This method will enable us to realise a data-driven implementation of projection-based fault detection as well. To illustrate and demonstrate the methods developed in our work, experimental study on the laboratory three-tank system and some achieved results will be finally presented.

### 3 Basic fault detection methods based on orthogonal projection

In this section, we apply orthogonal projection technique to achieving fault detection. Our major focus is on optimally detecting faults in dynamic systems with model uncertainties.

#### 3.1 Orthogonal projection-based residual generation

It is a known result (Georgiou, 1988) that the orthogonal projection onto the image subspace  $\mathcal{I}_G$  is given by

$$\mathcal{P}_{\mathcal{I}_G} = \mathcal{L}_{\mathcal{I}_G} \mathcal{L}_{\mathcal{I}_G}^*, \mathcal{L}_{\mathcal{I}_G}^* : \mathcal{H}_2 \rightarrow \mathcal{H}_2, \mathcal{L}_{\mathcal{I}_G}^* = \mathcal{P}_{\mathcal{H}_2} \mathcal{L}_{\mathcal{I}_G}^{\sim}. \quad (31)$$

Correspondingly, the projection of a data vector  $\begin{bmatrix} u \\ y \end{bmatrix} \in \mathcal{H}_2$  onto the image subspace is

$$p_{\mathcal{I}_G} = \mathcal{P}_{\mathcal{I}_G} \begin{bmatrix} u \\ y \end{bmatrix}.$$

The difference between  $\begin{bmatrix} u \\ y \end{bmatrix}$  and  $p_{\mathcal{I}_G}$  as its estimate,

$$\begin{bmatrix} u \\ y \end{bmatrix} - p_{\mathcal{I}_G} = (\mathcal{I} - \mathcal{P}_{\mathcal{I}_G}) \begin{bmatrix} u \\ y \end{bmatrix} = (\mathcal{I} - \mathcal{L}_{\mathcal{I}_G} \mathcal{P}_{\mathcal{H}_2} \mathcal{L}_{\mathcal{I}_G}^{\sim}) \begin{bmatrix} u \\ y \end{bmatrix}, \quad (32)$$

indicates how far the measurement (data) vector  $\begin{bmatrix} u \\ y \end{bmatrix}$  deviates from the nominal system dynamics expressed by the system SIR. Thus, its  $l_2$ -norm is the distance between the data vector and the image subspace. In this regard, we introduce the following definition.

**Definition 2** Given the model (1) and the corresponding operator  $\mathcal{L}_{\mathcal{I}_G}$ , system  $(\mathcal{I} - \mathcal{P}_{\mathcal{I}_G}) \begin{bmatrix} u \\ y \end{bmatrix}$  is called projection-based residual generator with output

$$r_{\mathcal{I}_G} = \begin{bmatrix} u \\ y \end{bmatrix} - p_{\mathcal{I}_G} = (\mathcal{I} - \mathcal{P}_{\mathcal{I}_G}) \begin{bmatrix} u \\ y \end{bmatrix} \quad (33)$$

as projection-based residual. The  $l_2$ -norm of  $r_{\mathcal{I}_G}$ ,

$$\|r_{\mathcal{I}_G}\|_2 = \text{dist} \left( \begin{bmatrix} u \\ y \end{bmatrix}, \mathcal{I}_G \right) \quad (34)$$

is the distance from  $\begin{bmatrix} u \\ y \end{bmatrix}$  to  $\mathcal{I}_G$ .

It should be remarked that  $\mathcal{I} - \mathcal{L}_{\mathcal{I}_G} \mathcal{P}_{\mathcal{H}_2} \mathcal{L}_{\mathcal{I}_G^\perp}$  defines the projection onto  $\mathcal{I}_G^\perp$ . That is

$$\begin{aligned} \mathcal{I}_G^\perp &= \left\{ r_{\mathcal{I}_G} : r_{\mathcal{I}_G} = (\mathcal{I} - \mathcal{L}_{\mathcal{I}_G} \mathcal{P}_{\mathcal{H}_2} \mathcal{L}_{\mathcal{I}_G^\perp}) \begin{bmatrix} u \\ y \end{bmatrix}, \begin{bmatrix} u \\ y \end{bmatrix} \in \mathcal{H}_2 \right\}, \\ \mathcal{H}_2 &= \mathcal{I}_G \oplus \mathcal{I}_G^\perp. \end{aligned}$$

In other words, the residual subspace is in fact  $\mathcal{I}_G^\perp$ . Under consideration of our study purpose, we prefer the term ‘‘residual’’ over projection onto the orthogonal complement of  $\mathcal{I}_G$ .

Remembering the natural relation between SKR and the residual generation as well as the known fact that  $\mathcal{K}_G = \mathcal{I}_G$  (Vinnicombe, 2000), it is of considerable interest to investigate relations among the operator  $\mathcal{L}_{\mathcal{I}_G}$ , the orthogonal projection  $\mathcal{P}_{\mathcal{I}_G}$  and the system SKR.

**Lemma 1** Let  $\mathcal{L}_{K_G}$  and  $\mathcal{L}_{K_G^\sim}$  be Laurent operators with symbol  $K_G$  and  $K_G^\sim$ , respectively. It holds

$$\mathcal{L}_{K_G^\sim} \mathcal{L}_{K_G} + \mathcal{L}_{\mathcal{I}_G} \mathcal{L}_{\mathcal{I}_G^\perp} = \mathcal{I}, \quad (35)$$

$$\mathcal{I} - \mathcal{P}_{\mathcal{H}_2} \mathcal{L}_{K_G^\sim} \mathcal{L}_{K_G} = \mathcal{P}_{\mathcal{I}_G} + \mathcal{P}_{\mathcal{H}_2} \mathcal{L}_{\mathcal{I}_G} \mathcal{P}_{\mathcal{H}_2^\perp} \mathcal{L}_{\mathcal{I}_G^\perp}. \quad (36)$$

**Proof.** Identity (35) is the result of

$$\begin{bmatrix} M_0^\sim & N_0^\sim \\ -\hat{N}_0 & \hat{M}_0 \end{bmatrix} \begin{bmatrix} M_0 & -\hat{N}_0^\sim \\ N_0 & \hat{M}_0^\sim \end{bmatrix} = \begin{bmatrix} M_0 & -\hat{N}_0^\sim \\ N_0 & \hat{M}_0^\sim \end{bmatrix} \begin{bmatrix} M_0^\sim & N_0^\sim \\ -\hat{N}_0 & \hat{M}_0 \end{bmatrix} = \begin{bmatrix} I & 0 \\ 0 & I \end{bmatrix}.$$

It follows from (35) that

$$\mathcal{P}_{\mathcal{H}_2} \mathcal{L}_{K_G^\sim} \mathcal{L}_{K_G} = \mathcal{P}_{\mathcal{H}_2} (\mathcal{I} - \mathcal{L}_{\mathcal{I}_G} \mathcal{L}_{\mathcal{I}_G^\perp}),$$

which yields

$$\begin{aligned} \mathcal{I} - \mathcal{P}_{\mathcal{H}_2} \mathcal{L}_{K_G^\sim} \mathcal{L}_{K_G} &= \mathcal{P}_{\mathcal{H}_2} \mathcal{L}_{\mathcal{I}_G} \mathcal{L}_{\mathcal{I}_G^\perp} = \mathcal{P}_{\mathcal{H}_2} \mathcal{L}_{\mathcal{I}_G} \mathcal{P}_{\mathcal{H}_2} \mathcal{L}_{\mathcal{I}_G^\perp} + \mathcal{P}_{\mathcal{H}_2} \mathcal{L}_{\mathcal{I}_G} \mathcal{P}_{\mathcal{H}_2^\perp} \mathcal{L}_{\mathcal{I}_G^\perp} \\ &= \mathcal{P}_{\mathcal{I}_G} + \mathcal{P}_{\mathcal{H}_2} \mathcal{L}_{\mathcal{I}_G} \mathcal{P}_{\mathcal{H}_2^\perp} \mathcal{L}_{\mathcal{I}_G^\perp}. \end{aligned}$$

Equation (36) illustrates that, although  $\mathcal{I} - \mathcal{P}_{\mathcal{H}_2} \mathcal{L}_{K_G^\sim} \mathcal{L}_{K_G}$  is a self adjoint operator that maps vectors in  $\mathcal{H}_2$  to  $\mathcal{H}_2$ , it is not a projection operator. The operator  $\mathcal{P}_{\mathcal{H}_2} \mathcal{L}_{\mathcal{I}_G} \mathcal{P}_{\mathcal{H}_2^\perp} \mathcal{L}_{\mathcal{I}_G^\perp}$  and relations (35)-(36) will play an important role in our subsequent work.

### 3.2 Residual generators and implementation algorithms

In this subsection, online computation issues of  $\|r_{\mathcal{I}_G}\|_2$  are addressed. It follows from (31) and (32) that

$$\|r_{\mathcal{I}_G}\|_2^2 = \left\| \begin{bmatrix} u \\ y \end{bmatrix} \right\|_2^2 - \left\| \mathcal{L}_{I_G} \mathcal{P}_{\mathcal{H}_2} \mathcal{L}_{I_G} \begin{bmatrix} u \\ y \end{bmatrix} \right\|_2^2 = \left\| \begin{bmatrix} u \\ y \end{bmatrix} \right\|_2^2 - \left\| \mathcal{P}_{\mathcal{H}_2} \mathcal{L}_{I_G} \begin{bmatrix} u \\ y \end{bmatrix} \right\|_2^2. \quad (37)$$

The relation

$$\mathcal{L}_{I_G} = \mathcal{P}_{\mathcal{H}_2} \mathcal{L}_{I_G} + \mathcal{P}_{\mathcal{H}_2^\perp} \mathcal{L}_{I_G}$$

leads to

$$\begin{aligned} \left\| \mathcal{P}_{\mathcal{H}_2} \mathcal{L}_{I_G} \begin{bmatrix} u \\ y \end{bmatrix} \right\|_2^2 &= \left\| \mathcal{L}_{I_G} \begin{bmatrix} u \\ y \end{bmatrix} \right\|_2^2 - \left\| \mathcal{P}_{\mathcal{H}_2^\perp} \mathcal{L}_{I_G} \begin{bmatrix} u \\ y \end{bmatrix} \right\|_2^2 \\ \implies \|r_{\mathcal{I}_G}\|_2^2 &= \left\| \begin{bmatrix} u \\ y \end{bmatrix} \right\|_2^2 - \left\| \mathcal{L}_{I_G} \begin{bmatrix} u \\ y \end{bmatrix} \right\|_2^2 + \left\| \mathcal{P}_{\mathcal{H}_2^\perp} \mathcal{L}_{I_G} \begin{bmatrix} u \\ y \end{bmatrix} \right\|_2^2. \end{aligned} \quad (38)$$

Operator

$$\mathcal{H}_{I_G} := \mathcal{P}_{\mathcal{H}_2^\perp} \mathcal{L}_{I_G} : \mathcal{H}_2 \rightarrow \mathcal{H}_2^\perp$$

is the so-called Hankel operator with symbol  $I_G$  (Francis, 1987) and serves as a filter. Given the state space representation of  $I_G$ ,

$$\xi(k-1) = \bar{A}\xi(k) + \bar{B} \begin{bmatrix} u(k) \\ y(k) \end{bmatrix}, \xi \in \mathbb{R}^n, \bar{A} = (A + BF_0)^T, \bar{B} = [ F_0^T \quad (C + DF)^T ], \quad (39)$$

$$\varsigma(k) = \bar{C}\xi(k) + \bar{D} \begin{bmatrix} u(k) \\ y(k) \end{bmatrix} \in \mathbb{R}^p, \bar{C} = B^T, \bar{D} = [ V_0^T \quad (DV_0)^T ] \quad (40)$$

with  $\varsigma(k)$  as the output of system  $I_G \begin{bmatrix} u \\ y \end{bmatrix}$ , the computation of  $\left\| \mathcal{L}_{I_G} \begin{bmatrix} u \\ y \end{bmatrix} \right\|_2$  is straightforward. Moreover,

$$\varsigma_{\mathcal{H}} := \mathcal{H}_{I_G} \begin{bmatrix} u \\ y \end{bmatrix}$$

can be computed by means of discrete convolution as follows

$$\varsigma_{\mathcal{H}}(k) = - \sum_{i=0}^{\infty} \bar{C} \bar{A}^{k+i} \bar{B} \begin{bmatrix} u(i) \\ y(i) \end{bmatrix}, k \in (-\infty, 0].$$

As demonstrated in (Francis, 1987),  $\varsigma_{\mathcal{H}}$  can also be written as

$$\varsigma_{\mathcal{H}}(k) = \left( \Psi_o \Psi_c \begin{bmatrix} u \\ y \end{bmatrix} \right) (k), k \in (-\infty, 0], \quad (41)$$

where  $\Psi_o$  and  $\Psi_c$ ,

$$\begin{aligned} \Psi_c \begin{bmatrix} u \\ y \end{bmatrix} &= - \sum_{i=0}^{\infty} \bar{A}^i \bar{B} \begin{bmatrix} u(i) \\ y(i) \end{bmatrix}, (\Psi_o x)(k) = \bar{C} \bar{A}^k x(k), k \in (-\infty, 0], \\ \implies \mathcal{H}_{I_G} &= \Psi_o \Psi_c, \end{aligned}$$

are controllability and observability operators, respectively.

Note that, according to (35) given in Lemma 1,  $\|r_{\mathcal{I}_G}\|_2$  can be written as

$$\begin{aligned}\|r_{\mathcal{I}_G}\|_2^2 &= \left\| \mathcal{L}_{K_G} \mathcal{L}_{K_G} \begin{bmatrix} u \\ y \end{bmatrix} \right\|_2^2 + \left\| \mathcal{P}_{\mathcal{H}_2^\perp} \mathcal{L}_{I_G} \begin{bmatrix} u \\ y \end{bmatrix} \right\|_2^2 \\ &= \left\| \mathcal{L}_{K_G} \begin{bmatrix} u \\ y \end{bmatrix} \right\|_2^2 + \left\| \mathcal{P}_{\mathcal{H}_2^\perp} \mathcal{L}_{I_G} \begin{bmatrix} u \\ y \end{bmatrix} \right\|_2^2.\end{aligned}\quad (42)$$

Recalling that  $\mathcal{L}_{K_G} \begin{bmatrix} u \\ y \end{bmatrix}$  is equivalent to the observer-based residual generator, i.e.

$$r_0 = \mathcal{L}_{K_G} \begin{bmatrix} u \\ y \end{bmatrix} = K_G \begin{bmatrix} u \\ y \end{bmatrix} = \begin{bmatrix} -\hat{N}_0 & \hat{M}_0 \end{bmatrix} \begin{bmatrix} u \\ y \end{bmatrix}, \quad (43)$$

it holds

$$\left\| \mathcal{L}_{K_G} \begin{bmatrix} u \\ y \end{bmatrix} \right\|_2 = \|r_0\|_2,$$

and thus

$$\|r_{\mathcal{I}_G}\|_2^2 = \|r_0\|_2^2 + \left\| \mathcal{P}_{\mathcal{H}_2^\perp} \mathcal{L}_{I_G} \begin{bmatrix} u \\ y \end{bmatrix} \right\|_2^2. \quad (44)$$

Equation (44) reveals the relation between the projection-based and observer-based residual generation. The latter, as well-known, is the state of the art technique for fault detection in dynamic systems. This fact motivates us to have a close look at the term

$$\left\| \mathcal{L}_{I_G} \mathcal{P}_{\mathcal{H}_2^\perp} \mathcal{L}_{I_G} \begin{bmatrix} u \\ y \end{bmatrix} \right\|_2 = \left\| \mathcal{P}_{\mathcal{H}_2^\perp} \mathcal{L}_{I_G} \begin{bmatrix} u \\ y \end{bmatrix} \right\|_2$$

that marks the difference between  $\|r_{\mathcal{I}_G}\|_2$  and  $\|r_0\|_2$ . Note that, on the one hand,

$$\mathcal{L}_{I_G} \mathcal{P}_{\mathcal{H}_2^\perp} \mathcal{L}_{I_G} \begin{bmatrix} u \\ y \end{bmatrix} \in \mathcal{L}_2 \text{ and } \mathcal{L}_{K_G} \mathcal{L}_{I_G} = 0. \quad (45)$$

Moreover,

$$\forall \begin{bmatrix} u \\ y \end{bmatrix} \in \mathcal{I}_G, \exists v \in \mathcal{H}_2, \text{ s.t. } \begin{bmatrix} u \\ y \end{bmatrix} = \mathcal{L}_{I_G} v,$$

which leads to

$$\mathcal{L}_{I_G} \mathcal{P}_{\mathcal{H}_2^\perp} \mathcal{L}_{I_G} \begin{bmatrix} u \\ y \end{bmatrix} = \mathcal{L}_{I_G} \mathcal{P}_{\mathcal{H}_2^\perp} \mathcal{L}_{I_G} \mathcal{L}_{I_G} v = 0.$$

On the other hand, for  $\begin{bmatrix} u \\ y \end{bmatrix} \in \mathcal{I}_G^\perp \subset \mathcal{H}_2$ , it is possible that

$$\mathcal{L}_{I_G} \mathcal{P}_{\mathcal{H}_2^\perp} \mathcal{L}_{I_G} \begin{bmatrix} u \\ y \end{bmatrix} \neq 0. \quad (46)$$

Relations (45)-(46) showcase that

- changes caused by  $\begin{bmatrix} u \\ y \end{bmatrix} \in \mathcal{I}_G^\perp \subset \mathcal{H}_2$  and satisfying (46) cannot be detected using an observer-based residual generator, since they do not lead to any variation in  $r_0$ ;

- in against, it is possible to detect these changes using  $r_{\mathcal{I}_G}$ , as described by (44).

In the context of fault detection, it can thus be claimed that the residual signal  $r_{\mathcal{I}_G}$  is more sensitive to faults than  $r_0$ .

Next, we address the interpretation of  $\left\| \mathcal{H}_{I_G} \begin{bmatrix} u \\ y \end{bmatrix} \right\|_2 = \left\| \mathcal{P}_{\mathcal{H}_2^\perp} \mathcal{L}_{I_G} \begin{bmatrix} u \\ y \end{bmatrix} \right\|_2$  from the fault detection aspect. To this end, consider the relation

$$\left\| \mathcal{H}_{I_G} \begin{bmatrix} u \\ y \end{bmatrix} \right\|_2 = \left\| \mathcal{H}_{I_G}^* \varsigma_{\mathcal{H}} \right\|_2, \varsigma_{\mathcal{H}} \in \mathcal{H}_2^\perp$$

where  $\mathcal{H}_{I_G}^*$  is the adjoint of  $\mathcal{H}_{I_G}$ . As demonstrated in (Francis, 1987), based on (41)  $\mathcal{H}_{I_G}^*$  can be written as

$$\mathcal{H}_{I_G}^* : \mathcal{H}_2^\perp \rightarrow \mathcal{H}_2, \mathcal{H}_{I_G}^* = (\Psi_o \Psi_c)^* = \Psi_c^* \Psi_o^*,$$

and correspondingly  $\mathcal{H}_{I_G}^* \varsigma_{\mathcal{H}}$  yields

$$x_0 = \Psi_o^* \varsigma_{\mathcal{H}} = \sum_{k=-\infty}^0 (\bar{A}^T)^k \bar{C}^T \varsigma_{\mathcal{H}}(k), \quad (47)$$

$$\begin{bmatrix} u(k) \\ y(k) \end{bmatrix} = (\Psi_c^* x_0)(k) = -\bar{B}^T (\bar{A}^T)^k x_0, k \in [0, \infty). \quad (48)$$

In this regard,  $\left\| \mathcal{P}_{\mathcal{H}_2^\perp} \mathcal{L}_{I_G} \begin{bmatrix} u \\ y \end{bmatrix} \right\|_2$  can be interpreted as the influence of deviations from the (nominal) image subspace in the past (i.e. over the time interval  $(-\infty, 0]$ ), which affects the dynamics of the residual generator  $(\mathcal{I} - \mathcal{P}_{\mathcal{I}_G}) \begin{bmatrix} u \\ y \end{bmatrix}$  in form of the response to the corresponding changes in initial condition (i.e. via  $x_0$ ).

Summarising the discussion on relation (44) and the interpretation of  $\left\| \mathcal{P}_{\mathcal{H}_2^\perp} \mathcal{L}_{I_G} \begin{bmatrix} u \\ y \end{bmatrix} \right\|_2$ , it can be concluded that the projection-based residual generator  $(\mathcal{I} - \mathcal{P}_{\mathcal{I}_G}) \begin{bmatrix} u \\ y \end{bmatrix}$  is not only efficient in detecting existing faults (i.e. over the time interval  $[0, \infty)$ ) like the observer-based residual generator  $\mathcal{L}_{K_G} \begin{bmatrix} u \\ y \end{bmatrix}$ , but also more capable of detecting faults in the past (i.e. over the time interval  $(-\infty, 0]$ ).

### 3.3 Threshold setting

We now consider threshold setting issues for systems with model uncertainty described by

$$G = NM^{-1} = (N_0 + \Delta_N)(M_0 + \Delta_M)^{-1}, I_G = \begin{bmatrix} M \\ N \end{bmatrix} = \begin{bmatrix} M_0 + \Delta_M \\ N_0 + \Delta_N \end{bmatrix} = I_{G_0} + \Delta_I, \quad (49)$$

$$I_{G_0} = \begin{bmatrix} M_0 \\ N_0 \end{bmatrix}, \Delta_I = \begin{bmatrix} \Delta_M \\ \Delta_N \end{bmatrix}$$

with normalised SIR  $I_G$ . It is assumed that

$$\sup \|\Delta_I\|_\infty = \delta_{\Delta_I} < 1, \quad (50)$$

**Remark 2** Hereafter, notation  $G_0$  is adopted for the nominal system transfer matrix, i.e. uncertainty- and fault-free system dynamics.

On the assumption of (50), threshold is set to prevent false alarms (Ding, 2008), namely during fault-free operations

$$J = \|r_{\mathcal{I}_G}\|_2 \leq J_{th}. \quad (51)$$

Recall that for some  $\Delta_I$ ,

$$\mathcal{I}_G = \left\{ \begin{bmatrix} u \\ y \end{bmatrix} : \begin{bmatrix} u \\ y \end{bmatrix} = \begin{bmatrix} M \\ N \end{bmatrix} v, v \in \mathcal{H}_2 \right\}$$

defines an image subspace that is obviously different from  $\mathcal{I}_{G_0}$ ,

$$\mathcal{I}_{G_0} = \left\{ \begin{bmatrix} u \\ y \end{bmatrix} : \begin{bmatrix} u \\ y \end{bmatrix} = \begin{bmatrix} M_0 \\ N_0 \end{bmatrix} v, v \in \mathcal{H}_2 \right\}.$$

Defining furthermore the following subspace in  $\mathcal{H}_2$ ,

$$\mathcal{I}_{G,\delta} := \{ \mathcal{I}_G : \|\Delta_I\|_\infty = \|I_G - I_{G_0}\|_\infty \leq \delta_{\Delta_I} \}, \quad (52)$$

threshold setting problem (51) can be equivalently written as

$$J_{th} = \sup_{\|\Delta_I\|_\infty \leq \delta_{\Delta_I}} J = \sup_{\mathcal{I}_G \in \mathcal{I}_{G,\delta}} \sup_{\begin{bmatrix} u \\ y \end{bmatrix} \in \mathcal{I}_G} \text{dist} \left( \begin{bmatrix} u \\ y \end{bmatrix}, \mathcal{I}_{G_0} \right). \quad (53)$$

In this regard, it becomes apparent that definition and computation of a metric to measure the difference between two image subspaces,  $\mathcal{I}_G$  and  $\mathcal{I}_{G_0}$ , are helpful for solving the threshold setting problem (51). To this end, we adopt the concept of gap metric defined in (28)-(29) that is widely applied in robust control theory (Vinnicombe, 2000; Feintuch, 1998).

**Definition 3** Let

$$\mathcal{I}_{G_i} = \left\{ \begin{bmatrix} u_i \\ y_i \end{bmatrix} : \begin{bmatrix} u_i \\ y_i \end{bmatrix} = \begin{bmatrix} M_i \\ N_i \end{bmatrix} v, v \in \mathcal{H}_2 \right\}, i = 1, 2,$$

be two image subspaces. The directed gap  $\vec{\delta}_{\mathcal{I}}(\mathcal{I}_{G_1}, \mathcal{I}_{G_2})$  and gap metric  $\delta_{\mathcal{I}}(\mathcal{I}_{G_1}, \mathcal{I}_{G_2})$  are respectively defined

$$\vec{\delta}_{\mathcal{I}}(\mathcal{I}_{G_1}, \mathcal{I}_{G_2}) = \sup_{\begin{bmatrix} u_1 \\ y_1 \end{bmatrix} \in \mathcal{I}_{G_1}} \inf_{\begin{bmatrix} u_2 \\ y_2 \end{bmatrix} \in \mathcal{I}_{G_2}} \frac{\left\| \begin{bmatrix} u_1 \\ y_1 \end{bmatrix} - \begin{bmatrix} u_2 \\ y_2 \end{bmatrix} \right\|_2}{\left\| \begin{bmatrix} u_1 \\ y_1 \end{bmatrix} \right\|_2} \quad (54)$$

$$= \sup_{\begin{bmatrix} u_1 \\ y_1 \end{bmatrix} \in \mathcal{I}_{G_1}, \left\| \begin{bmatrix} u_1 \\ y_1 \end{bmatrix} \right\|_2 = 1} \text{dist} \left( \begin{bmatrix} u_1 \\ y_1 \end{bmatrix}, \mathcal{I}_{G_2} \right), \quad (55)$$

$$\delta_{\mathcal{I}}(\mathcal{I}_{G_1}, \mathcal{I}_{G_2}) = \max \left\{ \vec{\delta}_{\mathcal{I}}(\mathcal{I}_{G_1}, \mathcal{I}_{G_2}), \vec{\delta}_{\mathcal{I}}(\mathcal{I}_{G_2}, \mathcal{I}_{G_1}) \right\}. \quad (56)$$

The computation of  $\delta_{\mathcal{I}}(\mathcal{I}_{G_i}, \mathcal{I}_{G_j})$  was intensively investigated, and one of the key results is that

$$\vec{\delta}_{\mathcal{I}}(\mathcal{I}_{G_i}, \mathcal{I}_{G_j}) = \inf_{Q \in \mathcal{H}_{\infty}} \left\| \begin{bmatrix} M_i \\ N_i \end{bmatrix} - \begin{bmatrix} M_j \\ N_j \end{bmatrix} Q \right\|_{\infty}, \quad (57)$$

i.e. the gap metric can be calculated by solving the model matching problem (MMP) on the right-hand side of (57) (Georgiou, 1988; Georgiou and Smith, 1990; Vinnicombe, 2000). Below, we briefly delineate (57) using the result given in Lemma 1. It follows from (29) that

$$\vec{\delta}_{\mathcal{I}}(\mathcal{I}_{G_i}, \mathcal{I}_{G_j}) = \|(\mathcal{I} - \mathcal{P}_{G_j}) \mathcal{P}_{G_i}\|.$$

Since, according to Lemma 1,

$$\begin{aligned} \mathcal{I} - \mathcal{P}_{\mathcal{I}_{G_j}} &= \mathcal{I} - \mathcal{L}_{\mathcal{I}_{G_j}} \mathcal{L}_{\mathcal{I}_{G_j}^{\sim}} + \mathcal{L}_{\mathcal{I}_{G_j}} \mathcal{P}_{\mathcal{H}_2^{\perp}} \mathcal{L}_{\mathcal{I}_{G_j}^{\sim}} = \mathcal{L}_{K_{G_j}^{\sim}} \mathcal{L}_{K_{G_j}} + \mathcal{L}_{\mathcal{I}_{G_j}} \mathcal{P}_{\mathcal{H}_2^{\perp}} \mathcal{L}_{\mathcal{I}_{G_j}^{\sim}} \\ &= \begin{bmatrix} \mathcal{L}_{K_{G_j}^{\sim}} & \mathcal{L}_{\mathcal{I}_{G_j}} \end{bmatrix} \begin{bmatrix} \mathcal{L}_{K_{G_j}} \\ \mathcal{P}_{\mathcal{H}_2^{\perp}} \mathcal{L}_{\mathcal{I}_{G_j}^{\sim}} \end{bmatrix}, \end{aligned}$$

where  $K_{G_j}$  is the normalised SKR of  $G_j$ , it yields

$$\vec{\delta}(\mathcal{I}_{G_i}, \mathcal{I}_{G_j}) = \left\| \begin{bmatrix} \mathcal{L}_{K_{G_j}^{\sim}} & \mathcal{L}_{\mathcal{I}_{G_j}} \end{bmatrix} \begin{bmatrix} \mathcal{L}_{K_{G_j}} \\ \mathcal{P}_{\mathcal{H}_2^{\perp}} \mathcal{L}_{\mathcal{I}_{G_j}^{\sim}} \end{bmatrix} \mathcal{L}_{\mathcal{I}_{G_i}} \mathcal{L}_{\mathcal{I}_{G_i}}^* \right\|.$$

Noting further

$$\mathcal{L}_{\mathcal{I}_{G_i}}^* \mathcal{L}_{\mathcal{I}_{G_i}} = \mathcal{I}, \begin{bmatrix} \mathcal{L}_{K_{G_j}^{\sim}} & \mathcal{L}_{\mathcal{I}_{G_j}} \end{bmatrix}^* \begin{bmatrix} \mathcal{L}_{K_{G_j}^{\sim}} & \mathcal{L}_{\mathcal{I}_{G_j}} \end{bmatrix} = \mathcal{I},$$

it turns out

$$\vec{\delta}(\mathcal{I}_{G_i}, \mathcal{I}_{G_j}) = \left\| \begin{bmatrix} \mathcal{L}_{K_{G_i}} \mathcal{L}_{\mathcal{I}_{G_i}} \\ \mathcal{P}_{\mathcal{H}_2^{\perp}} \mathcal{L}_{\mathcal{I}_{G_j}^{\sim}} \mathcal{L}_{\mathcal{I}_{G_i}} \end{bmatrix} \right\|. \quad (58)$$

In (Georgiou and Smith, 1990), it is proved that

$$\left\| \begin{bmatrix} \mathcal{L}_{K_{G_i}} \mathcal{L}_{\mathcal{I}_{G_i}} \\ \mathcal{P}_{\mathcal{H}_2^{\perp}} \mathcal{L}_{\mathcal{I}_{G_j}^{\sim}} \mathcal{L}_{\mathcal{I}_{G_i}} \end{bmatrix} \right\| = \inf_{Q \in \mathcal{H}_{\infty}} \|I_{G_i} - I_{G_j} Q\|_{\infty}. \quad (59)$$

Concerning the computation of MMP (57), there exist well-established algorithms, see e.g. (Francis, 1987).

Now, we are in the position to solve the threshold setting problem defined in (51) and its re-formulation (53). Since

$$\forall \begin{bmatrix} u \\ y \end{bmatrix} \in \mathcal{I}_G, \text{dist} \left( \begin{bmatrix} u \\ y \end{bmatrix}, \mathcal{I}_{G_0} \right) \leq \vec{\delta}_{\mathcal{I}}(\mathcal{I}_G, \mathcal{I}_{G_0}) \left\| \begin{bmatrix} u \\ y \end{bmatrix} \right\|_2,$$

it holds

$$\sup_{\begin{bmatrix} u \\ y \end{bmatrix} \in \mathcal{I}_G} \text{dist} \left( \begin{bmatrix} u \\ y \end{bmatrix}, \mathcal{I}_{G_0} \right) = \vec{\delta}_{\mathcal{I}}(\mathcal{I}_G, \mathcal{I}_{G_0}) \left\| \begin{bmatrix} u \\ y \end{bmatrix} \right\|_2. \quad (60)$$

Using the well-established result given in (Georgiou and Smith, 1990; Vinnicombe, 2000) that for  $0 < \delta_{\Delta_I} < 1$ ,

$$\begin{aligned}\mathcal{I}_{G,\delta} &= \{\mathcal{I}_G : \|\Delta_I\|_\infty = \|I_G - I_{G_0}\|_\infty \leq \delta_{\Delta_I}\} \\ &= \left\{ \mathcal{I}_G : \delta_{\mathcal{I}}(\mathcal{I}_G, \mathcal{I}_{G_0}) = \vec{\delta}_{\mathcal{I}}(\mathcal{I}_G, \mathcal{I}_{G_0}) \leq \delta_{\Delta_I} \right\},\end{aligned}\quad (61)$$

we further have

$$\begin{aligned}\sup_{\|\Delta_I\|_\infty \leq \delta_{\Delta_I}} J &= \sup_{\mathcal{I}_G \in \mathcal{I}_{G,\delta}} \sup_{\begin{bmatrix} u \\ y \end{bmatrix} \in \mathcal{I}_G} \text{dist} \left( \begin{bmatrix} u \\ y \end{bmatrix}, \mathcal{I}_{G_0} \right) \\ &= \sup_{\|\Delta_I\|_\infty \leq \delta_{\Delta_I}} \vec{\delta}_{\mathcal{I}}(\mathcal{I}_G, \mathcal{I}_{G_0}) \left\| \begin{bmatrix} u \\ y \end{bmatrix} \right\|_2 = \delta_{\Delta_I} \left\| \begin{bmatrix} u \\ y \end{bmatrix} \right\|_2.\end{aligned}\quad (62)$$

If  $\delta_{\Delta_I} \left\| \begin{bmatrix} u \\ y \end{bmatrix} \right\|_2$  serves as a threshold, the detection performance is determined by the ratio  $\frac{J_N}{\delta_{\Delta_I}}$  with the normalised residual  $J_N$ ,

$$J_N = \frac{\|r_{\mathcal{I}_G}\|_2}{\left\| \begin{bmatrix} u \\ y \end{bmatrix} \right\|_2},$$

since it holds

$$J - \delta_{\Delta_I} \left\| \begin{bmatrix} u \\ y \end{bmatrix} \right\|_2 > 0 \iff \frac{J_N}{\delta_{\Delta_I}} > 1.$$

It becomes clear that if  $\frac{J_N}{\delta_{\Delta_I}}$  is larger than but close to one, false alarms can be easily triggered, for instance, by noises in the system. In order to enhance the detection robustness, further improvement of threshold setting is made. Consider the relation

$$\forall \mathcal{I}_G \in \mathcal{I}_{G,\delta}, \|r_{\mathcal{I}_G}\|_2^2 \leq \delta_{\Delta_I}^2 \left\| \begin{bmatrix} u \\ y \end{bmatrix} \right\|_2^2.$$

It turns out that  $\forall \mathcal{I}_G \in \mathcal{I}_{G,\delta}$ ,

$$\begin{aligned}\|r_{\mathcal{I}_G}\|_2^2 &\leq \delta_{\Delta_I}^2 \left( \|r_{\mathcal{I}_G}\|_2^2 + \left\| \mathcal{P}_{\mathcal{I}_G} \begin{bmatrix} u \\ y \end{bmatrix} \right\|_2^2 \right) \iff \\ \|r_{\mathcal{I}_G}\|_2^2 &\leq \frac{\delta_{\Delta_I}^2}{1 - \delta_{\Delta_I}^2} \left\| \mathcal{P}_{\mathcal{I}_G} \begin{bmatrix} u \\ y \end{bmatrix} \right\|_2^2.\end{aligned}\quad (63)$$

Notice that

$$\mathcal{P}_{\mathcal{I}_G} \begin{bmatrix} u \\ y \end{bmatrix} \in \mathcal{I}_{G_0} \subset \mathcal{I}_{G,\delta}.$$

As a result, we have



**Theorem 1** *Given the model (1) with model uncertainty satisfying (49) and (50), and suppose that projection-based residual  $r_{\mathcal{I}_G}$  is used for the detection purpose, then the corresponding threshold defined by (51) is given by*

$$J_{th} = \frac{\delta_{\Delta_I}}{\sqrt{1 - \delta_{\Delta_I}^2}} \left\| \mathcal{P}_{\mathcal{I}_G} \begin{bmatrix} u \\ y \end{bmatrix} \right\|_2 \quad (64)$$

$$= \frac{\delta_{\Delta_I}}{\sqrt{1 - \delta_{\Delta_I}^2}} \left( \left\| \begin{bmatrix} u \\ y \end{bmatrix} \right\|_2^2 - \|r_{\mathcal{I}_G}\|_2^2 \right)^{1/2}. \quad (65)$$

**Proof.** *Since the inequality (63) holds for all  $\mathcal{I}_G \in \mathcal{I}_{G,\delta}$ , it is straightforward that*

$$J_{th} = \sup_{\|\Delta_I\|_\infty \leq \delta_{\Delta_I}} \|r_{\mathcal{I}_G}\|_2 = \frac{\delta_{\Delta_I}}{\sqrt{1 - \delta_{\Delta_I}^2}} \left\| \mathcal{P}_{\mathcal{I}_G} \begin{bmatrix} u \\ y \end{bmatrix} \right\|_2.$$

*The threshold setting (65) immediately follows from the relation*

$$\begin{aligned} \left\| \begin{bmatrix} u \\ y \end{bmatrix} \right\|_2^2 &= \left\| \mathcal{P}_{\mathcal{I}_G^\perp} \begin{bmatrix} u \\ y \end{bmatrix} \right\|_2^2 + \left\| \mathcal{P}_{\mathcal{I}_G} \begin{bmatrix} u \\ y \end{bmatrix} \right\|_2^2 \\ &= \|r_{\mathcal{I}_G}\|_2^2 + \left\| \mathcal{P}_{\mathcal{I}_G} \begin{bmatrix} u \\ y \end{bmatrix} \right\|_2^2. \end{aligned}$$

■

The threshold  $J_{th}$  given in the above theorem is driven by the online measurement and thus called adaptive threshold (Ding, 2008). More importantly, the adaptive threshold (64) (equivalently (65)) is more sensitive to faults, since, as indicated by (65), the threshold will decrease, as a fault occurs in the system and thus the residual increases. This observation motivates us to deepen our understanding of this important aspect. To this end, let

$$J_{th,N} := \sup_{\|\Delta_I\|_\infty \leq \delta_{\Delta_I}} J_N = \frac{\delta_{\Delta_I}}{\sqrt{1 - \delta_{\Delta_I}^2}} \left( 1 - \frac{\|r_{\mathcal{I}_G}\|_2^2}{\left\| \begin{bmatrix} u \\ y \end{bmatrix} \right\|_2^2} \right)^{1/2} \quad (66)$$

be the normalised threshold, and

$$\mathcal{F} = \left\{ \begin{bmatrix} u \\ y \end{bmatrix} \in \mathcal{H}_2, \|r_{\mathcal{I}_G}\|_2 > \delta_{\Delta_I} \left\| \begin{bmatrix} u \\ y \end{bmatrix} \right\|_2 \right\}. \quad (67)$$

While  $\mathcal{I}_{G,\delta}$  denotes the set of all data collected during fault-free operations,  $\mathcal{F}$  can be interpreted as data set corresponding to faulty operations.

**Theorem 2** *Given the model (1) with model uncertainty satisfying (49) and (50), and suppose that projection-based residual  $r_{\mathcal{I}_G}$  is generated, then we have*

$$\forall \begin{bmatrix} u \\ y \end{bmatrix} \in \mathcal{I}_G \subset \mathcal{I}_{G,\delta}, J_{th,N} \geq \delta_{\Delta_I}, \quad (68)$$

$$\forall \begin{bmatrix} u \\ y \end{bmatrix} \in \mathcal{F}, J_{th,N} < \delta_{\Delta_I}, \quad (69)$$

$$\forall \begin{bmatrix} u \\ y \end{bmatrix} \in \mathcal{F}, \frac{J_N}{J_{th,N}} > \frac{J_N}{\delta_{\Delta_I}} > 1. \quad (70)$$

**Proof.** Relation (68) follows directly from

$$\forall \begin{bmatrix} u \\ y \end{bmatrix} \in \mathcal{I}_G \subset \mathcal{I}_{G,\delta}, 1 - \frac{\|r_{\mathcal{I}_G}\|_2^2}{\left\| \begin{bmatrix} u \\ y \end{bmatrix} \right\|_2^2} \geq 1 - \delta_{\Delta_I}^2.$$

For all  $\begin{bmatrix} u \\ y \end{bmatrix}$  belonging to  $\mathcal{F}$ , definition (67) results in

$$1 - \frac{\|r_{\mathcal{I}_G}\|_2^2}{\left\| \begin{bmatrix} u \\ y \end{bmatrix} \right\|_2^2} < 1 - \delta_{\Delta_I}^2 \iff J_{th,N} < \delta_{\Delta_I},$$

$$\frac{J_N}{J_{th,N}} = \frac{J_N}{\delta_{\Delta_I}} \left( \frac{1 - \delta_{\Delta_I}^2}{1 - \frac{\|r_{\mathcal{I}_G}\|_2^2}{\left\| \begin{bmatrix} u \\ y \end{bmatrix} \right\|_2^2}} \right)^{1/2} > \frac{J_N}{\delta_{\Delta_I}} > 1.$$

The theorem is thus proved. ■

From (68)-(69) in Theorem 2 it becomes apparent that

- during fault-free operations, the normalised threshold  $J_{th,N}$  is higher than or equal to the upper-bound of the uncertainty  $\delta_{\Delta_I}$ , and
- it decreases, as a fault defined in sense of (67) occurs in the system, and becomes smaller than  $\delta_{\Delta_I}$ .
- More importantly, (70) indicates that all these faults can be detected with enhanced robustness thanks to the larger ratio  $\frac{J_N}{J_{th,N}}$ .

These properties reveal that the proposed projection-based threshold setting is of higher robustness, which is useful to reduce false alarms caused by noises. In Section 6, it will be demonstrated that the adaptive threshold setting (64) or the normalised threshold (66) results in better detection performance than the threshold setting adopted in the observer-based detection schemes (Li and Ding, 2020*a*; Li and Ding, 2020*b*).

## 4 Project-based fault detection in feedback control systems

Due to wide integration of feedback control loops in automatic control systems, fault detection in feedback control loops draws special attention in research of model-based fault detection in dynamic systems. In this section, we describe two fault detection schemes for feedback control systems, which are developed respectively on the basis of (i) projection onto the image subspace and (ii) projection onto the closed-loop image subspace of the feedback control system under consideration. This work also serves as examples for demonstrating the application of the basic projection-based fault detection scheme presented in the previous section.

## 4.1 System models and closed-loop dynamics

Consider a feedback control loop

$$y(z) = G(z)u(z), u(z) = K(z)y(z) + v(z) \quad (71)$$

with a dynamic output controller  $K$  and reference vector  $v$ . It is a well-known result that all stabilising controllers can be parameterised by

$$K(z) = - \left( X_0(z) - Q(z)\hat{N}_0(z) \right)^{-1} \left( Y_0(z) + Q(z)\hat{M}_0(z) \right) \quad (72)$$

$$= - \left( \hat{Y}_0(z) + M_0(z)Q(z) \right) \left( \hat{X}_0(z) - N_0(z)Q(z) \right)^{-1}, \quad (73)$$

where  $Q(z) \in \mathcal{RH}_\infty$  is the so-called parameter system, and  $(\hat{M}_0, \hat{N}_0)$  and  $(M_0, N_0)$  are the coprime pairs of the nominal transfer function  $G_0$ , which, together with  $(\hat{X}_0, \hat{Y}_0)$  and  $(X_0, Y_0)$ , are given in (5)-(9) (Zhou, 1998). Without loss of generality, it is assumed that  $F = F_0, L = L_0$ . Moreover, the extended form of Bezout identity (7) holds:

$$\begin{bmatrix} M_0 & U_0 \\ N_0 & V_0 \end{bmatrix} \begin{bmatrix} \hat{V}_0 & -\hat{U}_0 \\ -\hat{N}_0 & \hat{M}_0 \end{bmatrix} = \begin{bmatrix} I & 0 \\ 0 & I \end{bmatrix}, \quad (74)$$

$$\begin{bmatrix} \hat{V}_0 & \hat{U}_0 \end{bmatrix} = \begin{bmatrix} X_0 - Q\hat{N}_0 & -Y_0 - Q\hat{M}_0 \end{bmatrix}, \begin{bmatrix} U_0 \\ V_0 \end{bmatrix} = \begin{bmatrix} -\hat{Y}_0 - M_0Q \\ \hat{X}_0 - N_0Q \end{bmatrix}.$$

It turns out

$$\begin{aligned} \begin{bmatrix} u \\ y \end{bmatrix} &= \begin{bmatrix} I & -K \\ -G_0 & I \end{bmatrix}^{-1} \begin{bmatrix} I \\ 0 \end{bmatrix} v = \begin{bmatrix} \hat{V}_0 & \hat{U}_0 \\ -\hat{N}_0 & \hat{M}_0 \end{bmatrix}^{-1} \begin{bmatrix} \hat{V}_0 \\ 0 \end{bmatrix} v \\ &= \begin{bmatrix} M_0 & -U_0 \\ N_0 & V_0 \end{bmatrix} \begin{bmatrix} \hat{V}_0 \\ 0 \end{bmatrix} v = \begin{bmatrix} M_0 \\ N_0 \end{bmatrix} \hat{v}, \hat{v} = \hat{V}_0 v. \end{aligned} \quad (75)$$

Now, suppose that the plant is corrupted with uncertainty (49)-(50),

$$G = (N_0 + \Delta_N)(M_0 + \Delta_M)^{-1}, I_G = I_{G_0} + \Delta_I. \quad (76)$$

The closed-loop dynamics is governed by

$$\begin{bmatrix} u \\ y \end{bmatrix} = \begin{bmatrix} I & -K \\ -G & I \end{bmatrix}^{-1} \begin{bmatrix} I \\ 0 \end{bmatrix} v. \quad (77)$$

It is assumed that

$$\|\Delta_{I,c}\|_\infty \leq b < 1, \Delta_{I,c} = \begin{bmatrix} \hat{V}_0 & -\hat{U}_0 \\ -\hat{N}_0 & \hat{M}_0 \end{bmatrix} \begin{bmatrix} \Delta_M \\ \Delta_N \end{bmatrix}. \quad (78)$$

It is known that (78) is a sufficient condition for the closed-loop stability (Vinnicombe, 2000).

The following two lemmas are useful for our subsequent study.

**Lemma 2** *Given feedback control loop (77) with the plant model (76) and control law (72)-(73), it holds*

$$\begin{bmatrix} u \\ y \end{bmatrix} = \begin{bmatrix} M \\ N \end{bmatrix} (I + \Delta_1)^{-1} \hat{v}, \Delta_1 = \begin{bmatrix} \hat{V}_0 & -\hat{U}_0 \end{bmatrix} \begin{bmatrix} \Delta_M \\ \Delta_N \end{bmatrix} \in \mathcal{H}_\infty. \quad (79)$$

The proof of the above lemma is given in Appendix.

**Lemma 3** *(Georgiou and Smith, 1990) Given (78) and let*

$$\begin{bmatrix} \hat{V}_0 & -\hat{U}_0 \\ -\hat{N}_0 & \hat{M}_0 \end{bmatrix} \begin{bmatrix} \Delta_M \\ \Delta_N \end{bmatrix} = \begin{bmatrix} \Delta_1 \\ \Delta_2 \end{bmatrix}. \quad (80)$$

Then it holds

$$\|\Delta_2 (I + \Delta_1)^{-1}\|_\infty \leq \frac{b}{\sqrt{1 - b^2}}. \quad (81)$$

## 4.2 Application of the projection-based fault detection scheme

Based on the closed-loop dynamics, we first present a fault detection scheme based on the projection onto the system image subspace. Notice that

$$\hat{v} = \hat{V}_0 v, \hat{V}_0 \in \mathcal{RH}_\infty, \hat{V}_0^{-1} \in \mathcal{RL}_\infty.$$

Hence, there exists an invertible  $R_0(z) \in \mathcal{RH}_\infty$  so that

$$\left( \hat{V}_0 R_0 \right)^\sim \hat{V}_0 R_0 = I \implies I_{\bar{G}_0} = \begin{bmatrix} \bar{M}_0 \\ \bar{N}_0 \end{bmatrix} = \begin{bmatrix} M_0 \\ N_0 \end{bmatrix} \hat{V}_0 R_0$$

is a normalised SIR. Define

$$\mathcal{I}_{\bar{G}_0} =: \left\{ \begin{bmatrix} u \\ y \end{bmatrix} : \begin{bmatrix} u \\ y \end{bmatrix} = \begin{bmatrix} \bar{M}_0 \\ \bar{N}_0 \end{bmatrix} v, v \in \mathcal{H}_2 \right\}. \quad (82)$$

It follows from the results in Subsection 3.1 that the corresponding orthogonal projection is

$$\mathcal{P}_{\mathcal{I}_{\bar{G}_0}} = \mathcal{L}_{I_{\bar{G}_0}} \mathcal{L}_{I_{\bar{G}_0}}^*, p_{\mathcal{I}_{\bar{G}_0}} = \mathcal{P}_{\mathcal{I}_{\bar{G}_0}} \begin{bmatrix} u \\ y \end{bmatrix},$$

and the projection-based residual is generated by

$$r_{\mathcal{I}_{\bar{G}_0}} = \begin{bmatrix} u \\ y \end{bmatrix} - p_{\mathcal{I}_{\bar{G}_0}} = \left( \mathcal{I} - \mathcal{P}_{\mathcal{I}_{\bar{G}_0}} \right) \begin{bmatrix} u \\ y \end{bmatrix}. \quad (83)$$

Next, we determine the threshold following the procedure introduced in Subsection 3.3. Since  $\forall (\Delta_M, \Delta_N), (I + \Delta_1), (I + \Delta_1)^{-1} \in \mathcal{H}_\infty$ , it follows from Lemma 2 that

$$\mathcal{I}_G := \left\{ \begin{bmatrix} u \\ y \end{bmatrix} : \begin{bmatrix} u \\ y \end{bmatrix} = \begin{bmatrix} M \\ N \end{bmatrix} (I + \Delta_1)^{-1} \hat{V}_0 R_0 v, v \in \mathcal{H}_2 \right\} \quad (84)$$

builds a closed  $\mathcal{H}_2$  subspace and is different from  $\mathcal{I}_{\bar{G}_0}$ . For our purpose, the difference

$$\begin{bmatrix} M \\ N \end{bmatrix} (I + \Delta_1)^{-1} \hat{V}_0 R_0 - \begin{bmatrix} M_0 \\ N_0 \end{bmatrix} \hat{V}_0 R_0$$

should be specified. By means of the following steps,

$$\begin{aligned}
\begin{bmatrix} (M_o + \Delta_M)(I + \Delta_1)^{-1} \\ (N_o + \Delta_N)(I + \Delta_1)^{-1} \end{bmatrix} - \begin{bmatrix} M_0 \\ N_0 \end{bmatrix} &= \left( \begin{bmatrix} \Delta_M \\ \Delta_N \end{bmatrix} - \begin{bmatrix} M_0 \\ N_0 \end{bmatrix} \Delta_1 \right) (I + \Delta_1)^{-1} \\
&= \left( I - \begin{bmatrix} M_0 \\ N_0 \end{bmatrix} \begin{bmatrix} \hat{V}_0 & -\hat{U}_0 \end{bmatrix} \right) \begin{bmatrix} \Delta_M \\ \Delta_N \end{bmatrix} (I + \Delta_1)^{-1} \\
&= \begin{bmatrix} U_0 \\ V_0 \end{bmatrix} \begin{bmatrix} -\hat{N}_0 & \hat{M}_0 \end{bmatrix} \begin{bmatrix} \Delta_M \\ \Delta_N \end{bmatrix} (I + \Delta_1)^{-1} = \begin{bmatrix} U_0 \\ V_0 \end{bmatrix} \Delta_2 (I + \Delta_1)^{-1}, \tag{85}
\end{aligned}$$

we have

$$\begin{aligned}
&\begin{bmatrix} M \\ N \end{bmatrix} (I + \Delta_1)^{-1} \hat{V}_0 - \begin{bmatrix} M_0 \\ N_0 \end{bmatrix} \hat{V}_0 = \begin{bmatrix} U_0 \\ V_0 \end{bmatrix} \Delta_2 (I + \Delta_1)^{-1} \hat{V}_0 \\
\Rightarrow \begin{bmatrix} M \\ N \end{bmatrix} (I + \Delta_1)^{-1} \hat{V}_0 R_0 - \begin{bmatrix} \bar{M}_0 \\ \bar{N}_0 \end{bmatrix} &= \begin{bmatrix} U_0 \\ V_0 \end{bmatrix} \Delta_2 (I + \Delta_1)^{-1} \hat{V}_0 R_0 \\
&=: I_{\bar{G}} - I_{\bar{G}_0} = \Delta_{I_{\bar{G}_0}}.
\end{aligned}$$

By Lemma 3,

$$\|\Delta_2 (I + \Delta_1)^{-1}\|_\infty \leq \frac{b}{\sqrt{1 - b^2}},$$

it holds

$$\|\Delta_{I_{\bar{G}_0}}\|_\infty \leq \frac{\gamma b}{\sqrt{1 - b^2}}, \gamma = \left\| \begin{bmatrix} U_0 \\ V_0 \end{bmatrix} \right\|_\infty. \tag{86}$$

On the assumption that  $\|\Delta_{I_{\bar{G}_0}}\|_\infty < 1$ , applying the result in Theorem 1 yields

$$J_{th} = \frac{\gamma b}{\sqrt{1 - (1 + \gamma^2)b^2}} \left( \left\| \begin{bmatrix} u \\ y \end{bmatrix} \right\|_2^2 - \|r_{\mathcal{I}_{\bar{G}_0}}\|_2^2 \right)^{1/2}. \tag{87}$$

### 4.3 A closed-loop image subspace projection-based fault detection scheme

Consider the nominal closed-loop dynamics (75)

$$\begin{bmatrix} u \\ y \end{bmatrix} = \begin{bmatrix} M_0 \\ N_0 \end{bmatrix} \hat{v},$$

which can be, for instance, used to generate an extended residual vector,

$$\begin{bmatrix} r_u \\ r_y \end{bmatrix} = \begin{bmatrix} u \\ y \end{bmatrix} - \begin{bmatrix} M_0 \\ N_0 \end{bmatrix} \hat{v} \in \mathcal{H}_2^{p+m},$$

for the purpose of detecting cyber-attacks on feedback control systems and recovering control performance degradation (Ding, 2020; Ding *et al.*, 2022). This motivates us to propose a fault detection scheme based on the projection onto the image subspace of the feedback control system defined in the sequel.

It is obvious that  $\begin{bmatrix} M_0 \\ N_0 \end{bmatrix} \in \mathcal{RH}_\infty$  and  $\left(I, \begin{bmatrix} M_0 \\ N_0 \end{bmatrix}\right)$  builds a RCP of the transfer matrix  $G_c^0(z)$ ,

$$y = G_c^0 \hat{v}, G_c^0 = \begin{bmatrix} M_0 \\ N_0 \end{bmatrix} \implies \begin{bmatrix} \hat{v} \\ u \\ y \end{bmatrix} = \begin{bmatrix} I \\ M_0 \\ N_0 \end{bmatrix} \hat{v} \quad (88)$$

with the sub-index  $c$  standing for closed-loop. The state space model of  $G_c^0$  is given by

$$G_c^0 := (A_c, B_c, C_c, D_c) = \left( A + BF_0, BV_0, \begin{bmatrix} F_0 \\ C + DF_0 \end{bmatrix}, \begin{bmatrix} V_0 \\ DV_0 \end{bmatrix} \right).$$

Based on it, we have the following normalised SIR of  $G_c^0$ :

$$\begin{aligned} \begin{bmatrix} \hat{v} \\ u \\ y \end{bmatrix} &= I_{G_c^0} \hat{v} = \begin{bmatrix} M_{0,c} \\ N_{0,c} \end{bmatrix} \hat{v}, \\ M_{0,c} &= (A_c + B_c F_c, B_c V_c, F_c, V_c), N_{0,c} = (A_c + B_c F_c, B_c V_c, C_c + D_c F_c, D_c V_c), \\ F_c &= -(I + D_c^T D_c + B_c^T X B_c)^{-1} \Phi, \Phi = D_c^T C_c + B_c^T X A_c, \\ V_c &= (I + D_c^T D_c + B_c^T X B_c)^{-1/2} \Gamma, \Gamma^T \Gamma = I, \\ X &= A_c^T X A_c + C_c^T C_c - \Phi^T (I + D_c^T D_c + B_c^T X B_c)^{-1} \Phi, X > 0. \end{aligned}$$

It is well-known that between any two RCPs there exists a one-to-one mapping (Ding, 2020). In our case, it holds

$$I_{G_c^0} = \begin{bmatrix} M_{0,c} \\ N_{0,c} \end{bmatrix} = \begin{bmatrix} I \\ M_0 \\ N_0 \end{bmatrix} M_{0,c}, N_{0,c} = \begin{bmatrix} M_0 \\ N_0 \end{bmatrix} M_{0,c}. \quad (89)$$

**Definition 4** Given the close-loop model (88) and the corresponding RCP  $(M_{0,c}, N_{0,c})$ , the  $\mathcal{H}_2$  subspace  $\mathcal{I}_{G_c^0}$  defined by

$$\mathcal{I}_{G_c^0} = \left\{ \begin{bmatrix} \hat{v} \\ u \\ y \end{bmatrix} : \begin{bmatrix} \hat{v} \\ u \\ y \end{bmatrix} = \begin{bmatrix} M_{0,c} \\ N_{0,c} \end{bmatrix} \hat{v}, \hat{v} \in \mathcal{H}_2 \right\} \quad (90)$$

is called image subspace of the closed-loop.

**Remark 3** In the above definition, it is assumed that  $\hat{V}_0^{-1} \in \mathcal{RH}_\infty$ . Otherwise,  $\hat{v}$  will be substituted by  $v$  and  $\begin{bmatrix} M_0 \\ N_0 \end{bmatrix} \hat{V}_0$  is handled as done in the previous subsection without loss of generality.

Applying the basic projection-based residual generation scheme introduced in Section 3 results in

$$r_c = \begin{bmatrix} \hat{v} \\ u \\ y \end{bmatrix} - p_{\mathcal{I}_{G_c^0}}, p_{\mathcal{I}_{G_c^0}} = \mathcal{P}_{\mathcal{I}_{G_c^0}} \begin{bmatrix} \hat{v} \\ u \\ y \end{bmatrix} = \left( I - \mathcal{L}_{\mathcal{I}_{G_c^0}} \mathcal{L}_{\mathcal{I}_{G_c^0}}^* \right) \begin{bmatrix} \hat{v} \\ u \\ y \end{bmatrix} \quad (91)$$

with the residual vector  $r_c$ . In the next step, the threshold  $J_{th,c}$ ,

$$J_{th,c} = \sup_{\|\Delta_{I,c}\|_\infty \leq b} \|r_c\|_2,$$

is to be determined. It follows from Lemma 2 that in case of uncertainty  $\Delta_I$ ,

$$\begin{aligned} \begin{bmatrix} \hat{v} \\ u \\ y \end{bmatrix} &= \begin{bmatrix} I \\ M(I + \Delta_1)^{-1} \\ N(I + \Delta_1)^{-1} \end{bmatrix} \hat{v} = \begin{bmatrix} I \\ (M_0 + \Delta_M)(I + \Delta_1)^{-1} \\ (N_0 + \Delta_N)(I + \Delta_1)^{-1} \end{bmatrix} \hat{v} \\ &= \left( \begin{bmatrix} M_{0,c} \\ N_{0,c} \end{bmatrix} + \begin{bmatrix} 0 \\ \Delta_{N_{0,c}} \end{bmatrix} \right) M_{0,c}^{-1} \hat{v}, \\ \Delta_{N_{0,c}} &= \left( \begin{bmatrix} (M_0 + \Delta_M)(I + \Delta_1)^{-1} \\ (N_0 + \Delta_N)(I + \Delta_1)^{-1} \end{bmatrix} - \begin{bmatrix} M_0 \\ N_0 \end{bmatrix} \right) M_{0,c}. \end{aligned}$$

Recalling (85), it turns out

$$\begin{aligned} \begin{bmatrix} (M_0 + \Delta_M)(I + \Delta_1)^{-1} \\ (N_0 + \Delta_N)(I + \Delta_1)^{-1} \end{bmatrix} - \begin{bmatrix} M_0 \\ N_0 \end{bmatrix} &= \begin{bmatrix} U_0 \\ V_0 \end{bmatrix} \Delta_2 (I + \Delta_1)^{-1} \\ \implies \Delta_{N_{0,c}} &= \begin{bmatrix} U_0 \\ V_0 \end{bmatrix} \Delta_2 (I + \Delta_1)^{-1} M_{0,c}. \end{aligned}$$

Consider that  $M_{0,c}, M_{0,c}^{-1} \in \mathcal{RH}_\infty$  and thus

$$\begin{aligned} \mathcal{I}_{G_c} &= \left\{ \begin{bmatrix} \hat{v} \\ u \\ y \end{bmatrix} : \begin{bmatrix} \hat{v} \\ u \\ y \end{bmatrix} = \begin{bmatrix} I \\ M(I + \Delta_1)^{-1} \\ N(I + \Delta_1)^{-1} \end{bmatrix} \hat{v}, \hat{v} \in \mathcal{H}_2 \right\} \\ &= \left\{ \begin{bmatrix} \hat{v} \\ u \\ y \end{bmatrix} : \begin{bmatrix} \hat{v} \\ u \\ y \end{bmatrix} = \left( \begin{bmatrix} M_{0,c} \\ N_{0,c} \end{bmatrix} + \begin{bmatrix} 0 \\ \Delta_{N_{0,c}} \end{bmatrix} \right) \hat{v}, \hat{v} \in \mathcal{H}_2 \right\}. \end{aligned}$$

Now, let

$$I_{G_c} = \begin{bmatrix} M_{0,c} \\ N_{0,c} \end{bmatrix} + \begin{bmatrix} 0 \\ \Delta_{N_{0,c}} \end{bmatrix} \implies I_{G_c} - I_{G_c^0} = \begin{bmatrix} 0 \\ \Delta_{N_{0,c}} \end{bmatrix} =: \Delta_{I_{G_c}}. \quad (92)$$

By Lemma 3, it holds

$$\begin{aligned} \|\Delta_{I_{G_c}}\|_\infty &= \left\| \begin{bmatrix} U_0 \\ V_0 \end{bmatrix} \Delta_2 (I + \Delta_1)^{-1} M_{0,c} \right\|_\infty \leq \frac{\gamma b}{\sqrt{1 - b^2}} = \varepsilon, \\ \left\| \begin{bmatrix} U_0 \\ V_0 \end{bmatrix} \right\|_\infty \|M_{0,c}\|_\infty &\leq \left\| \begin{bmatrix} U_0 \\ V_0 \end{bmatrix} \right\|_\infty = \gamma. \end{aligned} \quad (93)$$

In the sequel, it is assumed that  $\varepsilon < 1$ .

Next, let  $\delta(\mathcal{I}_{G_c}, \mathcal{I}_{G_c^0})$  be the gap metric between  $\mathcal{I}_{G_c}$  and  $\mathcal{I}_{G_c^0}$ , and define

$$\begin{aligned} \mathcal{I}_{G_c, \Delta_{I_{G_c}}}(\varepsilon) &= \{ \mathcal{I}_{G_c} : \|\Delta_{I_{G_c}}\|_\infty = \|I_{G_c} - I_{G_c^0}\|_\infty \leq \varepsilon \}, \\ \mathcal{I}_{G_c, \delta}(\varepsilon) &= \{ \mathcal{I}_{G_c} : \delta(\mathcal{I}_{G_c}, \mathcal{I}_{G_c^0}) \leq \varepsilon \}. \end{aligned}$$

Since, following the well-established result given in (Georgiou and Smith, 1990; Vinnicombe, 2000),

$$\mathcal{I}_{G_c, \Delta_{I_{G_c}}}(\varepsilon) = \mathcal{I}_{G_c, \delta}(\varepsilon),$$

we finally have the following theorem.

**Theorem 3** *Given the control loop (71) with control law (72)-(73) and uncertainty  $\Delta_{I,c}$  satisfying (78). Suppose that projection-based residual generator (91) is used with residual vector  $r_c$ , then the corresponding threshold is given by*

$$J_{th,c} = \sup_{\|\Delta_{I,c}\|_\infty \leq b} \|r_c\|_2 = \frac{\gamma b}{\sqrt{1 - (1 + \gamma^2) b^2}} \left( \left\| \begin{bmatrix} \hat{v} \\ u \\ y \end{bmatrix} \right\|_2^2 - \|r_c\|_2^2 \right)^{1/2}, \quad (94)$$

where  $\gamma$  is a constant given in (93).

**Proof.** The proof is analogue to the one of Theorem 1 and thus omitted. ■

It is noteworthy that, for both detection schemes presented in this section, the influence of controller design on the detection performance can be clearly seen from the condition (78) and threshold setting. This reveals that, in order to enhance the fault detectability (by reducing the threshold), the norms of the LCP and RCP of the controller,  $\|[\hat{V}_0 \quad -\hat{U}_0]\|_\infty$  and  $\left\| \begin{bmatrix} U_0 \\ V_0 \end{bmatrix} \right\|_\infty$ , are to be set as small as possible. It is well-known from robust control theory that reducing  $\|[\hat{V}_0 \quad -\hat{U}_0]\|_\infty$  or/and  $\left\| \begin{bmatrix} U_0 \\ V_0 \end{bmatrix} \right\|_\infty$  increases the stability margin. This observation coincides with the result reported in (Li and Ding, 2020a; Li and Ding, 2020b).

## 5 Fault classification issues

In the observer-based fault diagnosis framework, fault detection and isolation are two major tasks and mainly handled with the aid of system analysis and observer design. They can be addressed in the context of fault classification as well. Roughly speaking, the task of fault classification is to determine to which class a fault belongs. In this section, projection-based methods and algorithms are applied to dealing with fault classification issues.

### 5.1 Fault detection: a binary classification scheme

In the previous sections, we have studied the basic projection-based fault detection methods whose basis is the nominal system model and information about model uncertainties. This is a typical one-class classification problem. When a system model (or data) for faulty operations, in addition to the nominal model, exists, fault detection can be achieved using both models. This is a binary fault classification task. It is evident that binary classification solutions, thanks to additional information, could considerably enhance the fault detection performance. Additionally, a multi-class classification problem towards fault isolation can be reformulated as a bank of binary fault classification sub-problems. In this subsection, binary fault classification issues are addressed in the framework of projection-based methods.

Consider  $G_i \in \mathcal{RL}_\infty^{m \times p}$ ,  $i = 0, 1$ , and let

$$K_{G_i} = \begin{bmatrix} -\hat{N}_i & \hat{M}_i \end{bmatrix}, I_{G_i} = \begin{bmatrix} M_i \\ N_i \end{bmatrix}$$



denote the corresponding normalised SKR and SIR of  $G_i$ , and  $\mathcal{K}_{G_i}, \mathcal{I}_{G_i}$  be the kernel and image subspaces,

$$\begin{aligned}\mathcal{K}_{G_i} &= \left\{ \begin{bmatrix} u \\ y \end{bmatrix} \in \mathcal{H}_2 : \mathcal{K}_i \begin{bmatrix} u \\ y \end{bmatrix} = 0 \right\}, \\ \mathcal{I}_{G_i} &= \left\{ \begin{bmatrix} u \\ y \end{bmatrix} : \begin{bmatrix} u \\ y \end{bmatrix} = \mathcal{I}_i v, v \in \mathcal{H}_2 \right\}.\end{aligned}$$

It is supposed that the system operates either in the nominal or faulty state, and the nominal and faulty models are represented by sub-index 0 and sub-index 1, respectively, i.e. any data vector  $\begin{bmatrix} u \\ y \end{bmatrix}$  belongs to  $\mathcal{I}_{G_0} \cup \mathcal{I}_{G_1}$ .

For the fault detection purpose, we now construct two projection-based residual generators,

$$\begin{aligned}\mathcal{P}_{\mathcal{I}_{G_i}} &= \mathcal{L}_{\mathcal{I}_{G_i}} \mathcal{L}_{\mathcal{I}_{G_i}}^*, p_{\mathcal{I}_{G_i}} = \mathcal{P}_{\mathcal{I}_{G_i}} \begin{bmatrix} u \\ y \end{bmatrix}, i = 0, 1, \\ r_{\mathcal{I}_{G_i}} &= \begin{bmatrix} u \\ y \end{bmatrix} - p_{\mathcal{I}_{G_i}} = \left( \mathcal{I} - \mathcal{L}_{\mathcal{I}_{G_i}} \mathcal{L}_{\mathcal{I}_{G_i}}^* \right) \begin{bmatrix} u \\ y \end{bmatrix}.\end{aligned}\quad (95)$$

It is evident that, without considering model uncertainties,

$$\begin{cases} r_{\mathcal{I}_{G_0}} = 0, \text{ fault-free,} \\ r_{\mathcal{I}_{G_1}} = 0, \text{ faulty.} \end{cases}$$

Consequently, the (ideal) detection logic seems to be

$$\begin{cases} \|r_{\mathcal{I}_{G_0}}\|_2 \leq J_{th,0} \Rightarrow \text{fault-free,} \\ \|r_{\mathcal{I}_{G_1}}\|_2 \leq J_{th,1} \Rightarrow \text{faulty,} \end{cases}\quad (96)$$

with  $J_{th,0}$  and  $J_{th,1}$  denoting the corresponding thresholds.

In order to study threshold setting for the residual generator (95), next, we analyse relations between  $\mathcal{P}_{\mathcal{I}_{G_i}}, i = 0, 1$ , and, associated with it, the dynamics of  $r_{\mathcal{I}_{G_i}}$ . Aiming at addressing practical cases, it is assumed that

$$0 < \vec{\delta}(\mathcal{I}_{G_0}, \mathcal{I}_{G_1}) = \vec{\delta}(\mathcal{I}_{G_1}, \mathcal{I}_{G_0}) = \delta(\mathcal{I}_{G_0}, \mathcal{I}_{G_1}) < 1.\quad (97)$$

The following theorem given by (Feintuch, 1998) (Theorem 9.1.4) is essential for our study.

**Theorem 4** *Suppose that  $\mathcal{V}_1$  and  $\mathcal{V}_2$  are two closed subspaces of  $\mathcal{H}$ . Then  $\delta(\mathcal{V}_1, \mathcal{V}_2) < 1$  if and only if operator  $\mathcal{P}_{\mathcal{V}_1} : \mathcal{V}_2 \rightarrow \mathcal{V}_1$  is one-to-one and onto.*

**Remark 4** *The proof given in (Feintuch, 1998) shows that*

$$\begin{aligned}\|\mathcal{P}_{\mathcal{V}_1} - \mathcal{P}_{\mathcal{V}_2}\| = \delta(\mathcal{V}_1, \mathcal{V}_2) < 1 &\implies \text{operator } (\mathcal{I} + \mathcal{P}_{\mathcal{V}_2} - \mathcal{P}_{\mathcal{V}_1}) \text{ is invertible,} \\ &\implies \mathcal{P}_{\mathcal{V}_1} \mathcal{H} = \mathcal{P}_{\mathcal{V}_1} (\mathcal{I} + \mathcal{P}_{\mathcal{V}_2} - \mathcal{P}_{\mathcal{V}_1}) \mathcal{H} = \mathcal{P}_{\mathcal{V}_1} \mathcal{P}_{\mathcal{V}_2} \mathcal{H}.\end{aligned}$$

*As a result,  $\mathcal{P}_{\mathcal{V}_1}$  maps  $\mathcal{V}_2$  to  $\mathcal{V}_1$  and it is one-to-one.*

Applying this theorem to our case results in the following corollary.

**Corollary 1** Given  $\mathcal{I}_{G_i}, i = 0, 1$ , and the corresponding projection operators  $\mathcal{P}_{\mathcal{I}_{G_i}}$ , then

$$\mathcal{I}_{G_i} \cap \mathcal{I}_{G_j} \neq \mathcal{O}, \quad (98)$$

$$\exists \begin{bmatrix} u \\ y \end{bmatrix} (\neq 0), \begin{bmatrix} u \\ y \end{bmatrix} \in \mathcal{I}_{G_i}, i = 0, 1 \implies r_{\mathcal{I}_{G_j}} = 0, j \neq i, \quad (99)$$

$$\begin{aligned} & \forall \begin{bmatrix} u \\ y \end{bmatrix} \in \mathcal{I}_{G_j}, \|r_{\mathcal{I}_{G_i}}\|_2 = \text{dist} \left( \begin{bmatrix} u \\ y \end{bmatrix}, \mathcal{I}_{G_i} \right) \\ & = \sqrt{\left\| \begin{bmatrix} u \\ y \end{bmatrix} \right\|_2^2 - \left\| \mathcal{P}_{\mathcal{I}_{G_i}} \mathcal{P}_{\mathcal{I}_{G_j}} \begin{bmatrix} u \\ y \end{bmatrix} \right\|_2^2} < \left\| \begin{bmatrix} u \\ y \end{bmatrix} \right\|_2, \end{aligned} \quad (100)$$

where  $\mathcal{O}$  denotes empty set.

**Proof.** The claim (98) is an immediate result of Theorem 4. From (98) follows (99). Equation in (100) is straightforward, because

$$\begin{aligned} \left\| \begin{bmatrix} u \\ y \end{bmatrix} \right\|_2^2 &= \left\| \mathcal{P}_{\mathcal{I}_{G_i}} \begin{bmatrix} u \\ y \end{bmatrix} \right\|_2^2 + \|r_{\mathcal{I}_{G_i}}\|_2^2, \\ \forall \begin{bmatrix} u \\ y \end{bmatrix} \in \mathcal{I}_{G_j}, \begin{bmatrix} u \\ y \end{bmatrix} &= \mathcal{P}_{\mathcal{I}_{G_j}} \begin{bmatrix} u \\ y \end{bmatrix}. \end{aligned}$$

The inequality is due to the fact that

$$\forall \begin{bmatrix} u \\ y \end{bmatrix}, \mathcal{P}_{\mathcal{I}_{G_i}} \mathcal{P}_{\mathcal{I}_{G_j}} \begin{bmatrix} u \\ y \end{bmatrix} \neq 0.$$

■

Observe that (100) implies,

$$\forall \begin{bmatrix} u \\ y \end{bmatrix} \in \mathcal{I}_{G_j}, \mathcal{P}_{\mathcal{I}_{G_i}} \begin{bmatrix} u \\ y \end{bmatrix} = \mathcal{P}_{\mathcal{I}_{G_i}} \mathcal{P}_{\mathcal{I}_{G_j}} \begin{bmatrix} u \\ y \end{bmatrix} \in \mathcal{I}_{G_i} \cap \mathcal{I}_{G_j},$$

that is, the projection of  $\begin{bmatrix} u \\ y \end{bmatrix}$  belonging to  $\mathcal{I}_{G_j}$  onto  $\mathcal{I}_{G_i}$  is a vector in the intersection set of  $\mathcal{I}_{G_j}$  and  $\mathcal{I}_{G_i}$ . Accordingly,  $\|r_{\mathcal{I}_{G_i}}\|_2$  reaches its largest value at  $\begin{bmatrix} u \\ y \end{bmatrix} \in \mathcal{I}_{G_j}$ , whose projection onto  $\mathcal{I}_{G_i} \cap \mathcal{I}_{G_j}$  is at the smallest value.

Consider that

$$\mathcal{I}_{G_i} = (\mathcal{I} - \mathcal{P}_{\mathcal{I}_{G_j}}) \mathcal{I}_{G_i} + \mathcal{P}_{\mathcal{I}_{G_j}} \mathcal{I}_{G_i}, \quad (101)$$

$$\mathcal{P}_{\mathcal{I}_{G_j}} \mathcal{I}_{G_i} = \mathcal{I}_{G_i} \cap \mathcal{I}_{G_j} \neq \mathcal{O}, (\mathcal{I} - \mathcal{P}_{\mathcal{I}_{G_j}}) \mathcal{I}_{G_i} \subseteq \mathcal{I}_{G_i}^\perp. \quad (102)$$

This means that the whole process data subspace,  $\mathcal{I}_G = \mathcal{I}_{G_0} \cup \mathcal{I}_{G_1}$ , consists of three sets,

$$\begin{aligned} \mathcal{I}_G &= \mathcal{S}_I \oplus \mathcal{S}_{II} \oplus \mathcal{S}_{III}, \quad (103) \\ \mathcal{S}_{II} &= \mathcal{I}_{G_0} \cap \mathcal{I}_{G_1}, \\ \mathcal{S}_I &= \left\{ \begin{bmatrix} u \\ y \end{bmatrix}, \begin{bmatrix} u \\ y \end{bmatrix} \in \mathcal{I}_{G_0} \cap \mathcal{I}_{G_1}^\perp \right\}, \\ \mathcal{S}_{III} &= \left\{ \begin{bmatrix} u \\ y \end{bmatrix}, \begin{bmatrix} u \\ y \end{bmatrix} \in \mathcal{I}_{G_1} \cap \mathcal{I}_{G_0}^\perp \right\}. \end{aligned}$$

Correspondingly, the dynamics of residuals  $r_{\mathcal{I}_{G_i}}, i = 0, 1$ , can be divided into three ranges indicating different operation states of the system:

$$\left\{ \begin{array}{l} \text{I. } 0 \leq \|r_{\mathcal{I}_{G_0}}\|_2 \leq J_{th,0} \text{ and } J_{th,1} < \|r_{\mathcal{I}_{G_1}}\|_2 \leq \delta(\mathcal{I}_{G_0}, \mathcal{I}_{G_1}) \left\| \begin{bmatrix} u \\ y \end{bmatrix} \right\|_2, \\ \text{II. } 0 \leq \|r_{\mathcal{I}_{G_0}}\|_2 \leq J_{th,0} \text{ and } 0 \leq \|r_{\mathcal{I}_{G_1}}\|_2 \leq J_{th,1}, \\ \text{III. } J_{th,0} < \|r_{\mathcal{I}_{G_0}}\|_2 \leq \delta(\mathcal{I}_{G_0}, \mathcal{I}_{G_1}) \left\| \begin{bmatrix} u \\ y \end{bmatrix} \right\|_2 \text{ and } 0 \leq \|r_{\mathcal{I}_{G_1}}\|_2 \leq J_{th,1}. \end{array} \right. \quad (104)$$

Here, the thresholds  $J_{th,0}$  and  $J_{th,1}$  are introduced to ensure a reliable detection in case of model uncertainties and thus can be determined using the gap metric schemes proposed in the previous sections. It is evident that Cases I and III, corresponding to  $\mathcal{S}_I$  and  $\mathcal{S}_{III}$ , respectively, indicate fault-free and faulty operations, respectively. Case II is the result of (99), which raises our interest for a reasonable and convincing interpretation.

It is well-known that faults caused by e.g. ageing is a longtime process. It begins with incipient degradation that does not affect the system dynamics significantly, and thus is interpreted as the transitional phase from the fault-free to faulty operation. Accordingly, the operations in this range can be called incipient fault. This is one interpretation of Case II. A further possible explanation for Case II is the so-called intermittent faults which repeatedly occur in the process over a time interval and then disappear. Their emergence and disappearance are activated, for instance, by certain system operation conditions. That means, in Case II, for some input signals (and so the corresponding outputs), the system may operate normally, and then, as a response to the change of input signals, works in the faulty operation. In summary, it can be concluded that, if the system operates in range II, warning should be triggered to call operator's attention for possible faults.

In order to gain a deeper insight into the above discussion, we would like to introduce some useful system theoretic aspects in the sequel. The following theorem is a summary of some relevant results in (Feintuch, 1998) (Section 9.1).

**Theorem 5** *Suppose that  $\mathcal{V}_1$  and  $\mathcal{V}_2$  are two closed subspaces of  $\mathcal{H}$ ,  $\delta(\mathcal{V}_1, \mathcal{V}_2) < 1$ , and the operator*

$$\mathcal{M}_{21} : \mathcal{V}_2 \rightarrow \mathcal{V}_1, \forall x \in \mathcal{V}_2, \mathcal{M}_{21}x = \mathcal{P}_{\mathcal{V}_1}x.$$

*is thus invertible. Then, it holds*

$$\begin{aligned} \mathcal{V}_2 &= (\mathcal{I}(\mathcal{V}_1) + \mathcal{X})\mathcal{V}_1, \\ \mathcal{X} : \mathcal{V}_1 &\rightarrow \mathcal{V}_1^\perp, \mathcal{X} = (\mathcal{I} - \mathcal{P}_{\mathcal{V}_1})\mathcal{M}_{21}^{-1}, \end{aligned}$$

*where  $\mathcal{I}(\mathcal{V}_1)$  is the identity operator restricted to  $\mathcal{V}_1$ .*

According to this theorem, we have, for instance,

$$\mathcal{I}_{G_1} = (\mathcal{I}(\mathcal{I}_{G_0}) + \mathcal{X})\mathcal{I}_{G_0}, \mathcal{X} = (\mathcal{I} - \mathcal{P}_{\mathcal{I}_{G_0}})\mathcal{M}_{10}^{-1}. \quad (105)$$

Equation (105) reveals the relation between fault-free and faulty subspaces. The subspace in  $\mathcal{I}_{G_1}$ , which is orthogonal to the (fault-free) subspace  $\mathcal{I}_{G_0}$  and thus the corresponding residual dynamics is represented by Case III in (104), is modelled by  $\mathcal{X}\mathcal{I}_{G_0}$ ,  $\mathcal{X} : \mathcal{I}_{G_0} \rightarrow \mathcal{I}_{G_0}^\perp$ . The transitional phase from the fault-free to faulty operation (Case II) is represented by

$\mathcal{I}_{G_1} - \mathcal{X}\mathcal{I}_{G_0}$ . Although it is difficult to give an analytical form of  $\mathcal{I}_{G_1} - \mathcal{X}\mathcal{I}_{G_0}$ , it is possible to characterise this subspace by means of simulation or data, for instance, using the so-called randomised algorithm technique (Ding *et al.*, 2019). This would be helpful to understand the mechanism of incipient and intermittent faults.

As a summary of this subsection, Figure 2 sketches the system operation state and the corresponding detection logic.

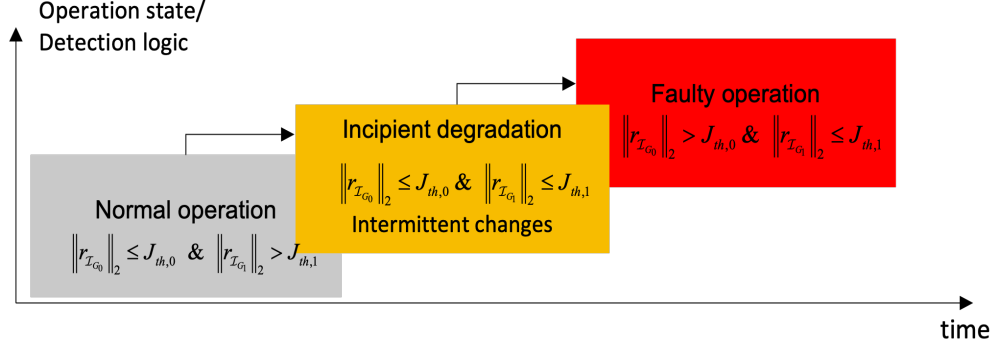


Figure 2: Operation states and detection logic

## 5.2 Fault isolation: multi-class classification

A straightforward extension of the binary classification method introduced in the previous subsection to multi-class classification provides us with a projection-based method for fault isolation. To this end, we first define fault classes under consideration. Let  $G_i \in \mathcal{RL}_\infty^{m \times p}$ ,  $i = 1, \dots, M$ , be (uncertain) transfer functions representing the  $M$  faulty classes of the nominal system (1), and  $\mathcal{K}_{G_i}, \mathcal{I}_{G_i}$  denote the corresponding kernel and image subspaces,

$$\mathcal{K}_{G_i} = \left\{ \begin{bmatrix} u \\ y \end{bmatrix} \in \mathcal{H}_2 : K_{G_i} \begin{bmatrix} u \\ y \end{bmatrix} = 0 \right\},$$

$$\mathcal{I}_{G_i} = \left\{ \begin{bmatrix} u \\ y \end{bmatrix} : \begin{bmatrix} u \\ y \end{bmatrix} = I_{G_i} v, v \in \mathcal{H}_2 \right\}.$$

Here,  $K_{G_i}$  and  $I_{G_i}$ ,  $i = 1, \dots, M$ , are the normalised SKR and SIR of  $G_i$ , which are known and defined by

$$K_{G_i} = \begin{bmatrix} -\hat{N}_i & \hat{M}_i \end{bmatrix}, I_{G_i} = \begin{bmatrix} M_i \\ N_i \end{bmatrix}.$$

Considering the existence of possible model uncertainties, let  $\Delta_{I_{G_i}}$ ,  $i = 1, \dots, M$ , denote uncertainties satisfying

$$\|\Delta_{I_{G_i}}\|_\infty \leq \delta_{I_i} < 1.$$

Recall that

$$\left\{ \begin{bmatrix} u \\ y \end{bmatrix} : \begin{bmatrix} u \\ y \end{bmatrix} = (I_{G_i} + \Delta_{I_{G_i}}) v, v \in \mathcal{H}_2, \|\Delta_{I_{G_i}}\|_\infty \leq \delta_{I_i} \right\}$$

$$= \{\mathcal{I}_{G_i} + \Delta\mathcal{I}_{G_i} : \delta(\mathcal{I}_{G_i}, \mathcal{I}_{G_i} + \Delta\mathcal{I}_{G_i}) \leq \delta_{I_i}\}.$$

This motivates us to define fault classifiability (isolability) as follows.

**Definition 5** Given fault classes  $G_i, i = 1, \dots, M$ . The  $j$ -th fault class with  $j \in \{1, \dots, M\}$  is called *classifiable*, if

$$\forall i \in \{1, \dots, M, i \neq j\}, \delta(\mathcal{I}_{G_i}, \mathcal{I}_{G_j}) > \max\{\delta_{I_i}, \delta_{I_j}\}. \quad (106)$$

The faults are called *classifiable* or *equivalently isolable*, if all fault classes are classifiable, i.e.

$$\forall i, j \in \{1, \dots, M\}, i \neq j, \delta(\mathcal{I}_{G_i}, \mathcal{I}_{G_j}) > \max\{\delta_{I_i}, \delta_{I_j}\}. \quad (107)$$

Condition (106) implies that the binary classification method introduced in the last subsection can be applied to classify (isolate) the  $j$ -th fault class. And, if this is true for all fault classes, as described by condition (107), then all faults are classifiable (isolable). In the sequel, on the assumption that the fault classes under consideration are classifiable, a fault classification algorithm is proposed. Suppose that

- process measurement data  $(u, y)$  have been collected and, based on them and by means of the projection-based detection algorithms proposed in Section 3, the fault has been detected,
- the collected data  $(u, y)$  as well as the projection-based binary fault classification method proposed in the last subsection are applied to the classification of the detected fault. The thresholds adopted in the classification algorithm are denoted by  $J_{th,i}, i = 1, \dots, M$ , where

$$J_{th,i} = \frac{\delta_{I_i}}{\sqrt{1 - \delta_{I_i}^2}} \left\| \mathcal{P}_{\mathcal{I}_{G_i}} \begin{bmatrix} u \\ y \end{bmatrix} \right\|_2 \quad (108)$$

following Theorem 1.

### Fault classification algorithm

- Generation of  $M$  projection-based residuals,

$$\begin{aligned} \mathcal{P}_{\mathcal{I}_{G_i}} &= \mathcal{L}_{\mathcal{I}_{G_i}} \mathcal{L}_{\mathcal{I}_{G_i}}^*, p_{\mathcal{I}_{G_i}} = \mathcal{P}_{\mathcal{I}_{G_i}} \begin{bmatrix} u \\ y \end{bmatrix}, i = 1, \dots, M, \\ r_{\mathcal{I}_{G_i}} &= \begin{bmatrix} u \\ y \end{bmatrix} - p_{\mathcal{I}_{G_i}} = \left( \mathcal{I} - \mathcal{L}_{\mathcal{I}_{G_i}} \mathcal{L}_{\mathcal{I}_{G_i}}^* \right) \begin{bmatrix} u \\ y \end{bmatrix}; \end{aligned}$$

- Decision logic

$$\left\| r_{\mathcal{I}_{G_j}} \right\|_2 \leq J_{th,j} \text{ and } \forall i \in \{1, \dots, M, i \neq j\}, J_{th,i} < \left\| r_{\mathcal{I}_{G_i}} \right\|_2 \leq \delta(\mathcal{I}_{G_j}, \mathcal{I}_{G_i}) \left\| \begin{bmatrix} u \\ y \end{bmatrix} \right\|_2 \quad (109)$$

$\implies$  the fault belongs to the  $j$ -th fault class,

$$\left\| r_{\mathcal{I}_{G_j}} \right\|_2 \leq J_{th,j} \text{ and } \exists i \in \{1, \dots, M, i \neq j\}, \left\| r_{\mathcal{I}_{G_i}} \right\|_2 \leq J_{th,i} \quad (110)$$

$\implies$  the fault belongs to both the  $j$ -th and  $i$ -th fault classes.

Next, we briefly explain the proposed algorithm. It is clear that in the first step, the measurement data  $(u, y)$  are first projected onto  $\mathcal{I}_{G_i}$  and, based on it, the residuals  $r_{\mathcal{I}_{G_i}}, i = 1, \dots, M$ , are generated. In the second step, by means of the decision logic (109) a decision is made to which fault class the measurement data  $(u, y)$  belong. As discussed in the last subsection, it is possible that the fault may simultaneously belong to more than one fault class. Accordingly, the rule (110) is introduced.

## 6 Two modified projection-based fault detection schemes

During real-time implementation of the projection-based residual generator (33), the following two problems may arise: (i) the involved online computation of  $\|r_{\mathcal{I}_G}\|_2$  as described by (38) or (42), and (ii) the (infinitely) long time interval required for the computation of  $l_2$ -norm of the residual signal. In this section, two alternative realisation schemes are proposed.

### 6.1 A fault detection scheme with projection onto $\mathcal{L}_2$ space

Comparing with a standard observer-based residual generation and evaluation makes it clear that the term  $\left\| \mathcal{P}_{\mathcal{H}_2^\perp} \mathcal{L}_{I_G} \begin{bmatrix} u \\ y \end{bmatrix} \right\|_2$  in the projection-based residual requires extra (online) computation in addition to the implementation of an observer. Moreover, the discussion in Section 3 reveals that this term is dedicated to detecting "past" faults in the (nominal) system image subspace. In other words, neglecting the term  $\left\| \mathcal{P}_{\mathcal{H}_2^\perp} \mathcal{L}_{I_G} \begin{bmatrix} u \\ y \end{bmatrix} \right\|_2$  could (considerably) reduce the online computation, although at the cost of missing detection of those faults in the set defined by  $\mathcal{L}_{I_G} \mathcal{P}_{\mathcal{H}_2^\perp} \mathcal{L}_{I_G} \begin{bmatrix} u \\ y \end{bmatrix}$ . In this subsection, we propose a projection-based scheme for the realisation of this trade-off strategy.

Remember that the first term of  $\|r_{\mathcal{I}_{G_0}}\|_2$  in (42) is the realisation of  $\mathcal{L}_{K_{G_0}^\sim} \mathcal{L}_{K_{G_0}}$ , which is an operator of the orthogonal projection given by

$$\mathcal{L}_{K_{G_0}^\sim} \mathcal{L}_{K_{G_0}} : \mathcal{L}_2 \rightarrow \mathcal{L}_2, \left( \mathcal{L}_{K_{G_0}^\sim} \mathcal{L}_{K_{G_0}} \right)^2 = \mathcal{L}_{K_{G_0}^\sim} \mathcal{L}_{K_{G_0}}.$$

Here,  $G_0$  represents the nominal system transfer matrix. It is clear that

$$\mathcal{P}_{\mathcal{K}_{G_0}}(\mathcal{L}_2) = \mathcal{I} - \mathcal{L}_{K_{G_0}^\sim} \mathcal{L}_{K_{G_0}} : \mathcal{L}_2 \rightarrow \mathcal{L}_2 \quad (111)$$

defines an orthogonal projection onto the kernel subspace  $\mathcal{K}_{G_0}$  in  $\mathcal{L}_2$ ,

$$\mathcal{K}_{G_0} = \left\{ \begin{bmatrix} u \\ y \end{bmatrix} \in \mathcal{L}_2 : \begin{bmatrix} -\hat{N}_0 & \hat{M}_0 \end{bmatrix} \begin{bmatrix} u \\ y \end{bmatrix} = 0 \right\},$$

and, accordingly,

$$r_{\mathcal{K}_{G_0}} = (\mathcal{I} - \mathcal{P}_{\mathcal{K}_{G_0}}) \begin{bmatrix} u \\ y \end{bmatrix} = \mathcal{L}_{K_{G_0}^\sim} \mathcal{L}_{K_{G_0}} \begin{bmatrix} u \\ y \end{bmatrix} \quad (112)$$

gives the implementation form of the residual vector. Consequently,

$$\|r_{\mathcal{K}_{G_0}}\|_2 = \left\| \mathcal{L}_{K_{G_0}^\sim} \mathcal{L}_{K_{G_0}} \begin{bmatrix} u \\ y \end{bmatrix} \right\|_2 = \left\| \mathcal{L}_{K_{G_0}} \begin{bmatrix} u \\ y \end{bmatrix} \right\|_2,$$

as expected. That means, for the detection purpose with the residual evaluation function  $\|r_{\mathcal{K}_{G_0}}\|_2$ , the needed online computation is the observer-based residual generator (10)-(12) or equivalently the SKR (43) leading to

$$\|r_0\|_2 = \|r_{\mathcal{K}_{G_0}}\|_2. \quad (113)$$

Next, we study threshold setting. Analogue to the uncertainty model (49)-(50), left-coprime factor uncertainty is introduced,

$$G = \hat{M}^{-1}\hat{N} = \left(\hat{M}_0 + \Delta_{\hat{M}}\right)^{-1} \left(\hat{N}_0 + \Delta_{\hat{N}}\right), \Delta_{\hat{N}}, \Delta_{\hat{M}} \in \mathcal{RH}_\infty, \quad (114)$$

$$K_G = \begin{bmatrix} -\hat{N} & \hat{M} \end{bmatrix} = \begin{bmatrix} -\hat{N}_0 - \Delta_{\hat{N}} & \hat{M}_0 + \Delta_{\hat{M}} \end{bmatrix} = K_{G_0} + \Delta_K, \quad (115)$$

$$K_{G_0} = \begin{bmatrix} -\hat{N}_0 & \hat{M}_0 \end{bmatrix}, \Delta_K = \begin{bmatrix} -\Delta_{\hat{N}} & \Delta_{\hat{M}} \end{bmatrix}, \sup \|\Delta_K\|_\infty = \delta_{\Delta_K} < 1 \quad (116)$$

with normalised SKR  $K_G$ . The threshold is defined by

$$J_{th} = \sup_{\|\Delta_K\|_\infty \leq \delta_{\Delta_K}} \|r_{\mathcal{K}_{G_0}}\|_2. \quad (117)$$

Notice that

$$r_0(z) = \begin{bmatrix} -\hat{N}_0(z) & \hat{M}_0(z) \end{bmatrix} \begin{bmatrix} u(z) \\ y(z) \end{bmatrix} = \begin{bmatrix} \Delta_{\hat{N}} & -\Delta_{\hat{M}} \end{bmatrix} \begin{bmatrix} u(z) \\ y(z) \end{bmatrix}, \quad (118)$$

which, thanks to (113), leads to,

$$\begin{aligned} \sup_{\|\Delta_K\|_\infty \leq \delta_{\Delta_K}} \|r_{\mathcal{K}_{G_0}}\|_2 &= \sup_{\|\Delta_K\|_\infty \leq \delta_{\Delta_K}} \|r_0\|_2 = \sup_{\|\Delta_K\|_\infty \leq \delta_{\Delta_K}} \left\| \begin{bmatrix} \Delta_{\hat{N}} & -\Delta_{\hat{M}} \end{bmatrix} \begin{bmatrix} u \\ y \end{bmatrix} \right\|_2 \\ &= \delta_{\Delta_K} \left\| \begin{bmatrix} u \\ y \end{bmatrix} \right\|_2. \end{aligned}$$

As a result, we have the following theorem.

**Theorem 6** *Given the model (1) with model uncertainty satisfying (114)-(116), and suppose that projection-based residual generator (118) is used for the detection purpose, then the corresponding threshold is given by*

$$J_{th} = \frac{\delta_{\Delta_K}}{\sqrt{1 - \delta_{\Delta_K}^2}} \left\| \mathcal{P}_{\mathcal{K}_{G_0}} \begin{bmatrix} u \\ y \end{bmatrix} \right\|_2 \quad (119)$$

$$= \frac{\delta_{\Delta_K}}{\sqrt{1 - \delta_{\Delta_K}^2}} \left( \left\| \begin{bmatrix} u \\ y \end{bmatrix} \right\|_2^2 - \|r_0\|_2^2 \right)^{1/2}. \quad (120)$$

**Proof.** The proof is similar to the one of Theorem 1. Hence, we only give the major step. It follows from

$$\begin{aligned} \forall \begin{bmatrix} u \\ y \end{bmatrix} \in \mathcal{K}_G &= \left\{ \begin{bmatrix} u \\ y \end{bmatrix} \in \mathcal{L}_2 : \begin{bmatrix} -\hat{N} & \hat{M} \end{bmatrix} \begin{bmatrix} u \\ y \end{bmatrix} = 0 \right\} \\ \|r_{\mathcal{K}_{G_0}}\|_2^2 &= \|r_0\|_2^2 \leq \delta_{\Delta_K}^2 \left\| \begin{bmatrix} u \\ y \end{bmatrix} \right\|_2^2 = \delta_{\Delta_K}^2 \left( \left\| \mathcal{P}_{\mathcal{K}_{G_0}} \begin{bmatrix} u \\ y \end{bmatrix} \right\|_2^2 + \|r_{\mathcal{K}_{G_0}}\|_2^2 \right) \end{aligned}$$

that

$$\begin{aligned} \|r_{\mathcal{K}_{G_0}}\|_2 = \|r_0\|_2 &\leq \frac{\delta_{\Delta_K}}{\sqrt{1 - \delta_{\Delta_K}^2}} \left\| \mathcal{P}_{\mathcal{K}_{G_0}} \begin{bmatrix} u \\ y \end{bmatrix} \right\|_2 \\ &= \frac{\delta_{\Delta_K}}{\sqrt{1 - \delta_{\Delta_K}^2}} \left( \left\| \begin{bmatrix} u \\ y \end{bmatrix} \right\|_2^2 - \|r_0\|_2^2 \right)^{1/2}. \end{aligned}$$

The proof is completed. ■

At the end of this subsection, we would like to compare the standard observer-based and the above introduced projection-based detection methods. In view of residual generation, the relation  $\|r_0\|_2 = \|r_{\mathcal{K}_G}\|_2$  implies that both methods are equivalent. From the information aspect, both residuals,  $r_0$  and  $r_{\mathcal{K}_G}$ , serve as a tool to gain information about changes in the system dynamics, and, in this regard, they contain the same information amount. This is the logic consequence of the intimate relation between the system kernel subspace and observer-based residual generation. Considering that the online computation cost for generating  $r_0$  is considerably lower than that for  $r_{\mathcal{K}_G}$ , it is reasonable to apply observer-based residual generator (118) for the residual generation purpose. It is noteworthy that, as a by-product, it provides us with an optimal observer-based solution for detecting faults in uncertain dynamic systems, a challenging issue as reported in (Li and Ding, 2020a; Li and Ding, 2020b). Concerning with threshold setting, notice that the basic idea of the existing observer-based methods, roughly speaking, consists in substituting  $y$  in the residual evaluation function by its upper-bound in the way

$$\begin{aligned} \|r_0\|_2 &= \left\| \begin{bmatrix} \Delta_{\hat{N}} & -\Delta_{\hat{M}} \end{bmatrix} \begin{bmatrix} u \\ y \end{bmatrix} \right\|_2 \leq \delta_{\Delta_K} \left\| \begin{bmatrix} u \\ y \end{bmatrix} \right\|_2 \leq \delta_{\Delta_K} (1 + \delta_y^2)^{1/2} \|u\|_2, \\ &\implies J_{th,r_0} := \delta_{\Delta_K} (1 + \delta_y^2)^{1/2} \|u\|_2, \end{aligned}$$

where  $J_{th,r_0}$  is the threshold, and

$$\|y\|_2 \leq \delta_y \|u\|_2$$

for some  $\delta_y > 0$  as an upper-bound of the system dynamics. In light of our discussion in Subsection 3.3 and calling that

$$\left\| \mathcal{P}_{\mathcal{K}_{G_0}} \begin{bmatrix} u \\ y \end{bmatrix} \right\|_2 \leq \left\| \begin{bmatrix} u \\ y \end{bmatrix} \right\|_2 \leq (1 + \delta_y^2)^{1/2} \|u\|_2,$$

it can be concluded that the threshold setting (119) of the projection-based method delivers better detection performance than the observer-based methods.

In a nutshell, comparing with existing observer-based schemes, the projection-based detection method proposed above offers better detection performance with identical online computations.

## 6.2 A projection-based fault detection over a finite time interval

In real applications, the  $l_2$ -norm (ref. to (24)) of the residual signal has to be approximately computed over a finite time interval. A reasonable solution of this concern is to substitute



the inner product definition given in (24) by

$$\langle x, y \rangle = \sqrt{\sum_{k=0}^N x^T(k)y(k)}, N < \infty, x, y \in \mathcal{H}_2.$$

Accordingly, the design of a projection-based residual generator should be performed in the framework of time-varying systems. This is a challenging topic and outside the scope of this work. Below, we propose a practical solution, which can be realised both in the model-based and data-driven fashions (Ding, 2014a; Ding, 2020).

For our purpose, we first introduce the following input-output (I/O) system model, which is achieved based on the (nominal) state space model (2)-(3) and widely adopted in subspace technique aided process identification and data-driven fault detection (Huang and Kadali, 2008; Ding, 2014a; Ding, 2020),

$$\begin{aligned} y_s(k) &= \Gamma_s L_p z_p + H_{u,s} u_s(k), z_p = \begin{bmatrix} u_p \\ y_p \end{bmatrix}, \\ y_s(k) &= \begin{bmatrix} y(k-s) \\ \vdots \\ y(k) \end{bmatrix} \in \mathbb{R}^{(s+1)m}, u_s(k) = \begin{bmatrix} u(k-s) \\ \vdots \\ u(k) \end{bmatrix} \in \mathbb{R}^{(s+1)p}, \\ y_p &= \begin{bmatrix} y(k-s-s_p) \\ \vdots \\ y(k-s-1) \end{bmatrix} \in \mathbb{R}^{s_p m}, u_p = \begin{bmatrix} u(k-s-s_p) \\ \vdots \\ u(k-s-1) \end{bmatrix} \in \mathbb{R}^{s_p p}, \\ \Gamma_s &= \begin{bmatrix} C \\ CA \\ \vdots \\ CA^s \end{bmatrix} \in \mathbb{R}^{(s+1)m \times n}, H_{u,s} = \begin{bmatrix} D & 0 \\ CB & \ddots & \ddots \\ \vdots & \ddots & \ddots & 0 \\ CA^{s-1}B & \cdots & CB & D \end{bmatrix} \in \mathbb{R}^{(s+1)m \times (s+1)p} \\ L_p &= [ A_K^{s_p-1} B_K \quad \cdots \quad B_K \quad A_K^{s_p-1} K \quad \cdots \quad K ], A_K = A - KC, B_K = B - KD, \end{aligned} \quad (121)$$

where  $K$  is the Kalman-filter or observer gain matrix, and  $s, s_p$  are two integers typically chosen larger than or equal to  $n$ . The reader is referred to, for instance, (Huang and Kadali, 2008; Ding, 2014a; Ding, 2020) for details about the above model. It is noteworthy that  $L_p z_p$  is a (good) approximation of the state vector  $x(k-s)$ .

Define

$$\mathcal{K}_G^{I/O} = \left\{ \begin{bmatrix} z_p \\ u_s(k) \\ y_s(k) \end{bmatrix} \in \mathbb{R}^{(s+s_p+1)(m+p)} : [ -\Gamma_s L_p \quad -H_{u,s} \quad I ] \begin{bmatrix} z_p \\ u_s(k) \\ y_s(k) \end{bmatrix} = 0 \right\}$$

as the kernel subspace of the I/O system model (121). Endowed with the inner product,

$$\begin{aligned} \langle \alpha, \beta \rangle &= \sum_{i=1}^{s+s_p+1} \alpha^T(i) \beta(i), \alpha = \begin{bmatrix} \alpha(1) \\ \vdots \\ \alpha(s+s_p+1) \end{bmatrix}, \beta = \begin{bmatrix} \beta(1) \\ \vdots \\ \beta(s+s_p+1) \end{bmatrix} \in \mathbb{R}^{(s+s_p+1)(m+p)}, \\ \langle \alpha, \alpha \rangle &=: \|\alpha\|, \end{aligned}$$

$\mathcal{K}_G^{I/O}$  builds a closed subspace in Hilbert space. It is straightforward that

$$\mathcal{P}_{\mathcal{K}_G^{I/O}} := I - K_{I/O}^T K_{I/O}, \quad (122)$$

$$K_{I/O} = \Sigma^{-1/2} \begin{bmatrix} -\Gamma_s L_p & -H_{u,s} & I \end{bmatrix}, \Sigma = \begin{bmatrix} -\Gamma_s L_p & -H_{u,s} & I \end{bmatrix} \begin{bmatrix} -(\Gamma_s L_p)^T \\ -H_{u,s}^T \\ I \end{bmatrix}$$

is an orthogonal projection onto  $\mathcal{K}_G^{I/O}$ . Analogue to Lemma 1,  $\mathcal{P}_{\mathcal{K}_G^{I/O}}$  has the following properties. Let

$$I_{I/O} = \begin{bmatrix} I & 0 \\ 0 & I \\ \Gamma_s L_p & H_{u,s} \end{bmatrix} \hat{\Sigma}^{-1/2}, \hat{\Sigma} = \begin{bmatrix} I & 0 & (\Gamma_s L_p)^T \\ 0 & I & H_{u,s}^T \end{bmatrix} \begin{bmatrix} I & 0 \\ 0 & I \\ \Gamma_s L_p & H_{u,s} \end{bmatrix}.$$

It holds

$$\begin{aligned} K_{I/O} I_{I/O} = 0, \begin{bmatrix} K_{I/O} \\ I_{I/O}^T \end{bmatrix} \begin{bmatrix} K_{I/O}^T & I_{I/O} \end{bmatrix} = \begin{bmatrix} I & 0 \\ 0 & I \end{bmatrix} \implies \\ \begin{bmatrix} K_{I/O}^T & I_{I/O} \end{bmatrix} \begin{bmatrix} K_{I/O} \\ I_{I/O}^T \end{bmatrix} = I \iff \mathcal{P}_{\mathcal{K}_G^{I/O}} = I - K_{I/O}^T K_{I/O} = I_{I/O} I_{I/O}^T. \end{aligned} \quad (123)$$

In fact,  $K_{I/O}$  and  $I_{I/O}$  are the normalised kernel and image representations of the I/O model (121). By means of  $\mathcal{P}_{\mathcal{K}_G^{I/O}}$ , a projection-based residual can be generated as follows

$$r_{I/O}(k) = (\mathcal{I} - \mathcal{P}_{\mathcal{K}_G^{I/O}}) \begin{bmatrix} z_p \\ u_s(k) \\ y_s(k) \end{bmatrix} = K_{I/O}^T K_{I/O} \begin{bmatrix} z_p \\ u_s(k) \\ y_s(k) \end{bmatrix}. \quad (124)$$

The corresponding evaluation function is

$$\|r_{I/O}(k)\| = \left\| K_{I/O}^T K_{I/O} \begin{bmatrix} z_p \\ u_s(k) \\ y_s(k) \end{bmatrix} \right\| = \left\| K_{I/O} \begin{bmatrix} z_p \\ u_s(k) \\ y_s(k) \end{bmatrix} \right\| = \|r_s(k)\|, \quad (125)$$

$$r_s(k) = K_{I/O} \begin{bmatrix} z_p \\ u_s(k) \\ y_s(k) \end{bmatrix} = \Sigma^{-1/2} (y_s(k) - \Gamma_s L_p z_p - H_{u,s} u_s(k)) \in \mathbb{R}^{(s+1)m}. \quad (126)$$

Equations (125)-(126) show that, for the detection purpose, generating  $r_s(k)$  is sufficient. It is known that the residual vector  $r_s(k)$  is widely used in the so-called parity space or data-driven methods (Ding, 2020).

Next, threshold setting is addressed. On the assumption that model uncertainties cause variations in the nominal system model and lead to

$$y_s(k) = (\Gamma_s L_p + \Delta_x) z_p + (H_{u,s} + \Delta_u) u_s(k), \quad (127)$$

$$\Delta K_{I/O} = \Sigma^{-1/2} \begin{bmatrix} -\Delta_x & -\Delta_u & 0 \end{bmatrix}, \quad (128)$$

$$\sup_{\Delta_x, \Delta_u} \|\Delta K_{I/O}\|_2 = \sup_{\Delta_x, \Delta_u} \bar{\sigma}(\Delta K_{I/O}) = \delta_{I/O} < 1 \quad (129)$$

with  $\Delta_x, \Delta_u$  representing the uncertainties, the threshold is set to be

$$J_{th} = \sup_{\|\Delta K_{I/O}\|_2 \leq \delta_{I/O}} \|r_{I/O}(k)\|.$$

Departing from the relations

$$\begin{aligned} \|r_{I/O}(k)\| &= \|r_s(k)\|, y_s(k) = (\Gamma_s L_p + \Delta_x) z_p + (H_{u,s} + \Delta_u) u_s(k) \\ r_s(k) &= \Sigma^{-1/2} (\Delta_x z_p + \Delta_u u_s(k)) = -\Delta K_{I/O} \begin{bmatrix} z_p \\ u_s(k) \\ y_s(k) \end{bmatrix}, \end{aligned}$$

and definitions

$$\begin{aligned} \mathcal{K}_{G,\Delta K}^{I/O} &= \left\{ \begin{bmatrix} z_p \\ u_s(k) \\ y_s(k) \end{bmatrix} : \begin{bmatrix} -\Gamma_s L_p - \Delta_x & -H_{u,s} - \Delta_u & I \end{bmatrix} \begin{bmatrix} z_p \\ u_s(k) \\ y_s(k) \end{bmatrix} = 0 \right\}, \\ \mathcal{K}_{G,\delta}^{I/O} &= \left\{ \mathcal{K}_{G,\Delta K}^{I/O} : \|\Delta K_{I/O}\|_2 \leq \delta_{I/O} \right\}, \end{aligned}$$

we have

$$\forall \begin{bmatrix} u \\ y \end{bmatrix} \in \mathcal{K}_{G,\Delta K}^{I/O} \subset \mathcal{K}_{G,\delta}^{I/O}, \|r_s(k)\| \leq \delta_{I/O} \left\| \begin{bmatrix} z_p \\ u_s(k) \\ y_s(k) \end{bmatrix} \right\|. \quad (130)$$

In the light of Theorem 1, the following theorem becomes obvious.

**Theorem 7** *Given the I/O model (121) with model uncertainty satisfying (127)-(129), and suppose that projection-based residual generator (124) and evaluation function (125) are used for the detection purpose, then the corresponding threshold is given by*

$$J_{th} = \frac{\delta_{I/O}}{\sqrt{1 - \delta_{I/O}^2}} \left\| \mathcal{P}_{\mathcal{K}_G^{I/O}} \begin{bmatrix} z_p \\ u_s(k) \\ y_s(k) \end{bmatrix} \right\| \quad (131)$$

$$= \frac{\delta_{I/O}}{\sqrt{1 - \delta_{I/O}^2}} \left( \left\| \begin{bmatrix} z_p \\ u_s(k) \\ y_s(k) \end{bmatrix} \right\|^2 - \|r_s(k)\|^2 \right)^{1/2}. \quad (132)$$

**Proof.** Since

$$\left\| \begin{bmatrix} z_p \\ u_s(k) \\ y_s(k) \end{bmatrix} \right\|^2 = \left\| \mathcal{P}_{\mathcal{K}_G^{I/O}} \begin{bmatrix} z_p \\ u_s(k) \\ y_s(k) \end{bmatrix} \right\|^2 + \|r_{I/O}(k)\|^2,$$

it follows from (130) that

$$\forall \begin{bmatrix} u \\ y \end{bmatrix} \in \mathcal{K}_{G,\Delta K}^{I/O} \subset \mathcal{K}_{G,\delta}^{I/O}, \|r_s(k)\|^2 \leq \delta_{I/O}^2 \left( \left\| \mathcal{P}_{\mathcal{K}_G^{I/O}} \begin{bmatrix} z_p \\ u_s(k) \\ y_s(k) \end{bmatrix} \right\|^2 + \|r_{I/O}(k)\|^2 \right),$$

which leads to (131) and (132). ■

## 7 An experimental study

### 7.1 Description of the experimental system

Due to their typical characteristics of a chemical process, three-tank systems are widely accepted as a benchmark process in laboratories for process control and fault diagnosis. The three-tank system used in our experimental study is laboratory setup TTS20, whose model and the model parameters are summarised as follows (Ding, 2020):

$$\begin{aligned}\mathcal{A}\dot{h}_1 &= Q_1 - Q_{13}, \mathcal{A}\dot{h}_2 = Q_2 + Q_{32} - Q_{20}, \mathcal{A}\dot{h}_3 = Q_{13} - Q_{32}, \\ Q_{13} &= a_1 s_{13} \text{sgn}(h_1 - h_3) \sqrt{2g|h_1 - h_3|}, \\ Q_{32} &= a_3 s_{23} \text{sgn}(h_3 - h_2) \sqrt{2g|h_3 - h_2|}, Q_{20} = a_2 s_0 \sqrt{2gh_2},\end{aligned}$$

where  $Q_1, Q_2$  are incoming mass flow ( $\text{cm}^3/\text{s}$ ),  $Q_{ij}$  is the mass flow ( $\text{cm}^3/\text{s}$ ) from the  $i$ -th tank to the  $j$ -th tank,  $h_i(t), i = 1, 2, 3$ , are the water level (cm) in the  $i$ -th tank and measurement variables, and  $s_{13} = s_{23} = s_0 = s_n$ .

Table 1: Parameters of TTS20

Parameters	Symbol	Value	Unit
cross section area of tanks	$\mathcal{A}$	154	$\text{cm}^2$
cross section area of pipes	$s_n$	0.5	$\text{cm}^2$
max. height of tanks	$H_{max}$	62	cm
max. flow rate of pump 1	$Q_{1_{max}}$	100	$\text{cm}^3/\text{s}$
max. flow rate of pump 2	$Q_{2_{max}}$	100	$\text{cm}^3/\text{s}$
coeff. of flow for pipe 1	$a_1$	0.45	
coeff. of flow for pipe 2	$a_2$	0.60	
coeff. of flow for pipe 3	$a_3$	0.45	

For our purpose of testing the projection-based fault detection schemes, the above nonlinear model is linearised at the operating point  $h_1 = 30\text{cm}$ ,  $h_2 = 20\text{cm}$ ,  $h_3 = 24\text{cm}$  and discretised with a sampling time equal to 5s. The resulted nominal model is given by

$$\begin{aligned}x(k+1) &= Ax(k) + Bu(k), x(k) = \begin{bmatrix} h_1(k) \\ h_2(k) \\ h_3(k) \end{bmatrix}, y(k) = \begin{bmatrix} x_1(k) \\ x_2(k) \end{bmatrix}, u(k) = \begin{bmatrix} Q_1(k) \\ Q_2(k) \end{bmatrix}, \\ A &= \begin{bmatrix} 0.9272 & -0.0012 & 0.0605 \\ -0.0064 & 0.8829 & 0.0561 \\ 0.0645 & 0.0632 & 0.8695 \end{bmatrix}, B = \begin{bmatrix} 0.03126 & -0.0000 \\ -0.0001 & 0.0305 \\ 0.0011 & 0.0011 \end{bmatrix}.\end{aligned}$$

In order to regulate the water level in tank 1 and tank 2, an observer-based state feedback controller is adopted,

$$\hat{x}(k+1) = (A - LC)\hat{x}(k) + Bu(k) + Ly(k), \quad (133)$$

$$u(k) = F\hat{x}(k) + v(k), \quad (134)$$

where  $F, L$  are designed using LQ optimal control and Kalman filter algorithms, respectively, which results in

$$F = \begin{bmatrix} -8.8470 & -0.0663 & -1.3821 \\ -0.0406 & -7.8259 & -1.1961 \end{bmatrix}, L = \begin{bmatrix} 0.7125 & 0.0213 \\ 0.0070 & 0.7202 \\ 0.0661 & 0.0917 \end{bmatrix}. \quad (135)$$

$v$  is the reference signal that is set corresponding to the operating point  $h_1 = 30\text{cm}$ ,  $h_2 = 20\text{cm}$  and given by

$$v(k) = \begin{bmatrix} 323.2805 \\ 219.1368 \end{bmatrix}.$$

## 7.2 Design of fault detection systems

The main objective of experimental test is to compare detection performance of observer-based and projection-based fault detection systems. To this end, three fault detection systems are designed as follows:

- A projection-based detection system, as proposed in Subsection 6.1. According to the relation

$$\|r_{\mathcal{K}_{G_0}}\|_2 = \|r_0\|_2,$$

the residual generation is realised using an observer-based residual generator with the observer gain  $L_0$  and post filter  $W_0$  computed by means of (18) and (19), which results in

$$L_0 = \begin{bmatrix} 0.0094 & 0.0015 \\ 0.0015 & 0.0046 \\ 0.0046 & 0.0024 \end{bmatrix}, W_0 = \begin{bmatrix} 0.9951 & -0.0008 \\ -0.0008 & 0.9974 \end{bmatrix}.$$

The computation of  $\|r_0\|_2$  is approximated by

$$\|r_0\|_2 = \left( \sum_{i=k}^{k+120} r_0^T(k+i)r_0(k+i) \right)^{1/2}$$

with a moving evaluation window. As discussed in Subsection 3.3, the residual evaluation function is built by a normalisation of  $r_0$ ,

$$J_N = \frac{\|r_0\|_2}{\left\| \begin{bmatrix} u \\ y \end{bmatrix} \right\|_2} = \left( \frac{\sum_{i=k}^{k+120} r_0^T(k+i)r_0(k+i)}{\sum_{i=k}^{k+120} (u^T(k+i)u(k+i) + y^T(k+i)y(k+i))} \right)^{1/2}.$$

The corresponding threshold is set following Theorem 6 and by means of a normalisation,

$$J_{th,N} = \frac{\delta_{\Delta_K}}{\sqrt{1 - \delta_{\Delta_K}^2}} (1 - J_N^2)^{1/2}.$$

To determine an upper-bound of left-coprime factor uncertainty  $\Delta_K$  (refer to (114)-(116))  $\delta_{\Delta_K}$ , possible variations from  $\pm 3.3\%$  in the system parameters  $\mathcal{A}, s_n, a_1, a_2, a_3$  are considered, which leads to

$$\Delta_K = \begin{bmatrix} -\Delta_{\hat{N}} & \Delta_{\hat{M}} \end{bmatrix}, \|\Delta_K\|_\infty \leq \delta_{\Delta_K} = 0.052.$$

- An observer-based fault detection system. Here, the Kalman filter applied in the observer-based controller is used for residual generation, with gain matrix  $L$  given by (135), and the generated residual is denoted by

$$r_{0,k}(k) = y(k) - C\hat{x}(k).$$

The threshold is set using the algorithm given in Theorem 2 (Li and Ding, 2020a),

$$J_{th,k} = \frac{\beta\delta_{\Delta_K}}{1 - \delta_{\Delta_K}b} \|v\|_2, \|v\|_2 = \left( \sum_{i=k}^{k+120} v^T(k+i)v(k+i) \right)^{1/2},$$

where

$$\beta = \|(I - C(zI - A + LC)^{-1}(L - L_0)) W_0^{-1}\|_{\infty} = 1.6257, b = \left\| \begin{bmatrix} U_0 \\ V_0 \end{bmatrix} \right\|_{\infty} = 7.9179,$$

$(V_0, U_0)$  is the normalised RCP of the controller (133)-(134) (refer to (74)).

- An observer-based fault detection system, which consists of an observer-based residual generator whose SKR, different from a Kalman filter, is normalised with  $L_0, W_0$  as the observer gain matrix and post-filter. As a result, it delivers  $r_0$  as the residual signal. Similar to the above observer-based fault detection system, the threshold setting is achieved using the algorithm given in Theorem 2 (Li and Ding, 2020a), which leads to

$$J_{th} = \frac{\delta_{\Delta_K}}{1 - \delta_{\Delta_K}b} \|v\|_2, \|v\|_2 = \left( \sum_{i=k}^{k+120} v^T(k+i)v(k+i) \right)^{1/2}.$$

### 7.3 Experimental results and analysis

To test the proposed projection-based fault detection system and compare it with the existing observer-based ones, the following two faults are realised directly on the laboratory setup TTS20:

- a 5% leakage fault in tank 1,
- a 7% plugging fault in pipe 1 (connecting tank 1 and tank 3).

Figures 3 - 8 show the test results. In detail,

- the top figure in Figure 3 gives the responses of the residual evaluation function  $J_N$  and the threshold  $J_{th,N}$  during fault-free operation over the time interval [1500s, 2150s] and faulty operation (5% leakage) over [2150s, 4000s]. A successful fault detection is achieved. The threshold  $J_{th,N}$  is shown in the bottom figure to demonstrate that it decreases as the residual increases;
- Figure 4 shows the residual evaluation function  $\|r_0\|_2$  and the threshold  $J_{th}$  over the same intervals with the 5% leakage fault. A successful fault detection is demonstrated as well;

- the top figure in Figure 5 showcases the residual evaluation function  $\|r_{0,k}\|_2$  and the threshold  $J_{th,k}$  over the same intervals with the 5% leakage fault, and demonstrates, together with the bottom figure, that the fault cannot be detected;
- Figures 6 - 8 give, analogue to Figures 3 - 5, the responses of the residual evaluation functions  $J_N, \|r_0\|_2, \|r_{0,k}\|_2$  and the corresponding thresholds  $J_{th,N}, J_{th}, J_{th,k}$  during fault-free operation over the time interval [2500s, 4000s] and faulty operation (7% plugging) over [4000s, 6500s], respectively. It is apparent that the fault can be successfully detected by the projection-based detection system, while both observer-based detection systems fail.

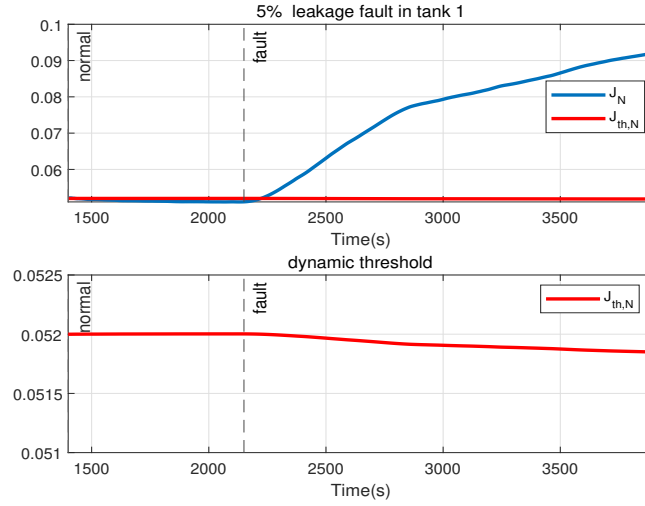


Figure 3: Detection of a leakage fault in tank 1 using the projection-based detection system

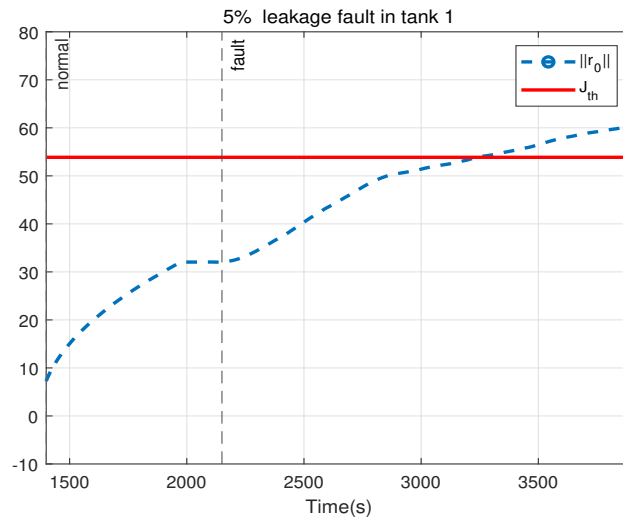


Figure 4: Detection of a leakage fault in tank 1 using the observer-based detection system (a normalised SKR)

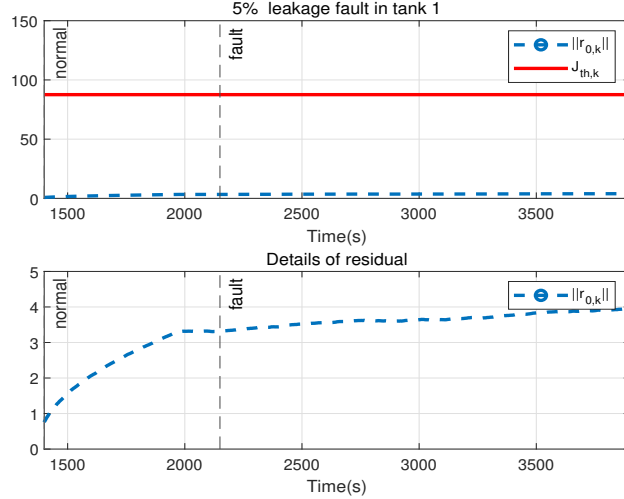


Figure 5: Detection of a leakage fault in tank 1 using the observer-based detection system (Kalman filter-based)

Next, we briefly analyse the above experimental results. The first conclusion is that the Kalman filter-based detection system is less capable of dealing with robust fault detection, when model uncertainties exists. The major reason lies in the residual generator setting. Recall that the projection-based method proposed in Subsection 6.1 leads to the normalised SKR as the (optimal) setting of the residual generator. From the system analysis point of view, (Ding, 2020) (Subsection 9.2.3) illustrates and verifies this conclusion. The normalised SKR is *co-inner* (Ding, 2020), that is, all singular values of SKR from the input pair  $(u, y)$  to the residual  $r_0$  are identically equal to 1. Checking the relation

$$r_{0,k}(z) = R(z)r_0(z), R(z) = (I - C(zI - A + LC)^{-1}(L - L_0)) W_0^{-1}$$

and the maximal and minimal singular values of  $R(z)$ ,

$$\sigma_{\max}(R) = \|R(z)\|_{\infty} = 1.6257, \sigma_{\min}(R) = 0.0556,$$

reveals that the Kalman filter-based residual generation is far away from optimal. We would like to emphasise that (Ding *et al.*, 2000) has proved that an optimal residual generation is achieved if the transfer function matrix from the input to the residual is *co-inner*.

Comparing the results in Figures 3 and 4 as well as 6 and 7 demonstrates obviously that the projection-based detection system is more sensitive to the faults than the observer-based one. Since both detection systems have the same residual generator, i.e. the normalised SKR, the different threshold settings are the result of the different detection performance. To put it in a nutshell, it can be concluded that the projection-based detection methods result in optimal fault detection performance.

## 8 Concluding remarks

In the previous sections, we have presented fault diagnosis schemes in the projection-based framework, including the basic fault detection (one-class classification) scheme, two detection methods for feedback control systems, binary and multi-class fault classification methods



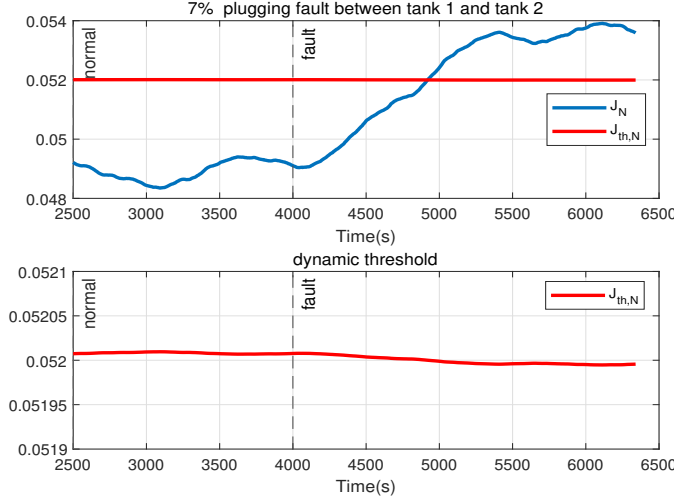


Figure 6: Detection of a plugging fault in pipe 1 using the projection-based detection system

towards fault detection and isolation, as well as two modified fault detection methods. Although they have been developed for different application purposes under possibly different system configuration assumptions, they have one point in common, namely the corresponding fault diagnosis system design follows the uniform procedure with the steps: (i) definition and determination of an orthogonal projection operator, (ii) construction of the projection-based residual generator and realisation of online implementation algorithm, mainly consisting of an observer plus, possibly, an additional filter, and (iii) gap metric-based threshold settings. All these results are summarised in Theorems 1-3 and 6-7. It is remarkable that all resulted fault diagnosis systems are optimal with respect to the classification distance metric, and the above design procedure can be applied both in the model-based and data-driven fashions. So far, the basic targets of our work, as described in Introduction, have been successfully reached.

Moreover, we have illustrated the major differences between the projection-based and observer-based fault detection schemes, and demonstrated the advantage of the projection-based scheme in enhancing fault detectability. In this context, a modified approach has also been proposed for the design of projection-based fault detection systems that are comparable with observer-based ones with regard to the online computation and offer better detection performance.

In our study on projection-based binary (fault) classification, it has been revealed that there generally exists an overlapping subspace of fault-free and faulty operations, which is described by an one-to-one mapping between the image subspaces of the fault-free and faulty system dynamics. This result is helpful for us to understand mechanisms of incipient and intermittent faults. Accordingly, an optimal classification scheme has been proposed, which is also the basic algorithm for multi-class fault classification (fault isolation).

Our work in this paper has focused on detecting and isolating multiplicative faults in dynamic systems with (multiplicative/parametric) uncertainties, motivated by the fact that there exist no general and systematic solutions for the relevant issues. It is natural to raise a question if projection-based methods can be applied to systems with additive disturbances (unknown

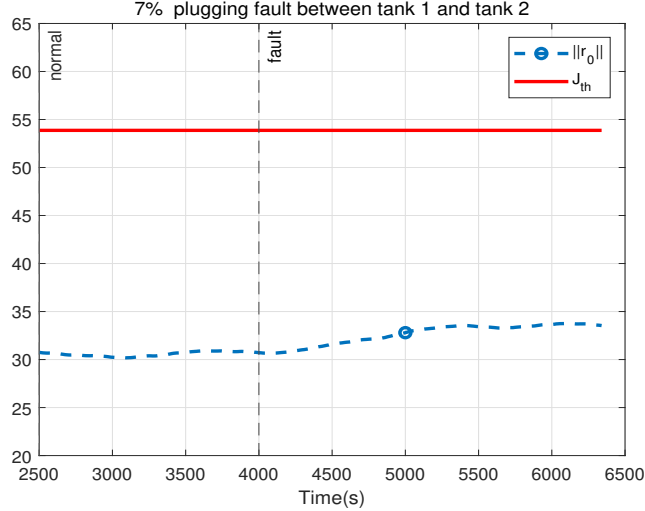


Figure 7: Detection of a plugging fault in pipe 1 using the observer-based detection system (a normalised SKR)

inputs) and faults. Below, we briefly illustrate such a case. For our purpose, consider the nominal model (2)-(3) with  $l_2$ -norm bounded unknown input vector  $d \in \mathbb{R}^{k_d}$ , and unknown fault vector  $f \in \mathbb{R}^{k_f}$ ,

$$x(k+1) = Ax(k) + Bu(k) + E_f f(k) + E_d d(k), \quad (136)$$

$$y(k) = Cx(k) + Du(k) + F_f f(k) + F_d d(k), \|d\|_2 \leq \delta_d, \quad (137)$$

where  $E_d, F_d, E_f, F_f$  are known matrices and  $\delta_d$  is the known upper bound. The corresponding optimal fault detection problem has been extensively studied (Hou and Patton, 1996; Ding *et al.*, 2000; Wang *et al.*, 2007). In order to compare with the existing results, we only consider projection  $\mathcal{P}_{\mathcal{K}_G}$  defined by (111) and assume that

$$\forall \theta \in [0, 2\pi], \text{rank} \begin{bmatrix} A - e^{j\theta} I & E_d \\ C & F_d \end{bmatrix} = n + m. \quad (138)$$

It turns out

$$\|r_{\mathcal{K}_G}\|_2 = \left\| \mathcal{L}_{\mathcal{K}_{G_0}} \begin{bmatrix} u \\ y \end{bmatrix} \right\|_2 = \|r_0\|_2. \quad (139)$$

It is well-known (Ding, 2008) that

$$\begin{aligned} r_0(z) &= \hat{M}_0(z)y(z) - \hat{N}_0(z)u(z) = \hat{N}_d(z)d(z), \\ \hat{N}_d(z) &= (A - LC, E_d - LF_d, WC, WF_d) \in \mathcal{RH}_\infty. \end{aligned}$$

Consequently, the threshold is set to be (Frank and Ding, 1994)

$$J_{th} = \sup_{\|d\|_2 \leq \delta_d} \|r_0\|_2 = \left\| \hat{N}_d \right\|_\infty \delta_d. \quad (140)$$

On the other hand, it is known that the above threshold setting is considerably conservative (Ding, 2008). Alternatively, we introduce a projection-based method to improve the threshold setting. Note that

$$\mathcal{R}_d = \left\{ d \in \mathcal{L}_2 : \hat{N}_d d \neq 0 \right\}$$

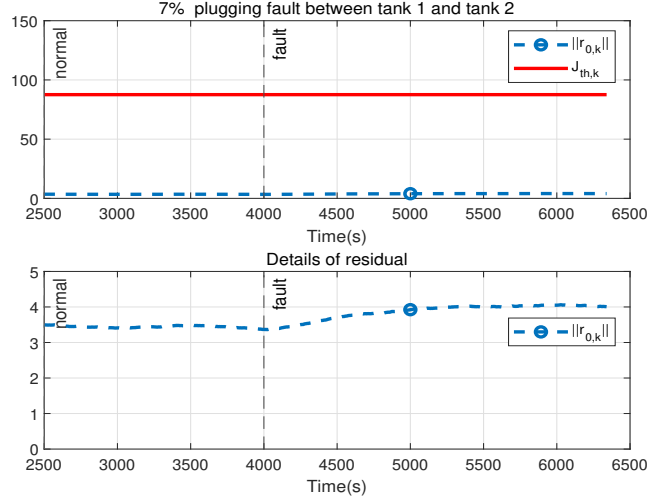


Figure 8: Detection of a plugging fault in pipe 1 using the observer-based detection system (Kalman filter-based)

is a subspace in  $\mathcal{L}_2$ , and the orthogonal projection of  $d$  onto  $\mathcal{R}_d$  is given by

$$\mathcal{P}_{\mathcal{R}_d} : \mathcal{L}_2 \rightarrow \mathcal{L}_2, \mathcal{P}_{\mathcal{R}_d} = \mathcal{L}_{\hat{N}_{d,0}} \mathcal{L}_{\hat{N}_{d,0}}^{-1}, \hat{N}_{d,0}(z) \hat{N}_{d,0}^{-1}(z) = I$$

with  $\hat{N}_{d,0}$  satisfying (Ding, 2008)

$$\hat{N}_{d,0}(z) = (A - L_d C, E_d - L_d F_d, W_d C, W_d F_d), \quad (141)$$

$$L_d = (A X C^T + E_d F_d^T) (C X C^T + F_d F_d^T)^{-1}, W_d = (C X C^T + F_d F_d^T)^{-1/2}, \quad (142)$$

$$X = A X A^T + E_d E_d^T - L_d (C X C^T + F_d F_d^T) L_d^T.$$

As shown in (Ding, 2008), there exists a post-filter  $R(z)$  so that

$$\begin{aligned} R \hat{N}_d &= \hat{N}_{d,0} \implies R r_0 = \hat{N}_{d,0} d =: \bar{r}_0, \\ R(z) &= (A - L_d C, (L_d - L) W^{-1}, -W_d C, W_d W^{-1}) \in \mathcal{RH}_\infty. \end{aligned}$$

Note that

$$\|\mathcal{P}_{\mathcal{R}_d} d\|_2 = \|\hat{N}_{d,0} d\|_2 = \|\bar{r}_0\|_2, \forall d \in \mathcal{R}_d, \|\mathcal{P}_{\mathcal{R}_d} d\|_2 = \|d\|_2. \quad (143)$$

The second equation in (143) leads to

$$J_{th} = \sup_{\|d\|_2 \leq \delta_d} \|\bar{r}_0\|_2 = \delta_d. \quad (144)$$

To demonstrate that  $\bar{r}_0$  delivers a better fault detection performance in comparison with  $r_0$ , it is sufficient to check  $\|\bar{r}_0\|_2$  vs.  $\|r_0\|_2 / \|\hat{N}_d\|_\infty$ , i.e. on the condition of the same threshold equal to  $\delta_d$ . It can be seen that

$$\gamma \|r_0\|_2 = \gamma \|\hat{N}_d d\|_2 \leq \|d\|_2 = \|\bar{r}_0\|_2, \gamma = \frac{1}{\|\hat{N}_d\|_\infty}.$$

This implies that  $\bar{r}_0$  delivers higher fault detectability than  $\gamma r_0$ .

We would like to call the reader's attention that the above fault detection system with the residual generator (141)-(142) and threshold (144) is the so-called unified solution (Ding *et al.*, 2000; Ding, 2008), which can be iteratively approached using linear matrix inequality solutions (Hou and Patton, 1996; Wang *et al.*, 2007). The above result gives a geometric solution and interpretation of optimal detection for systems with additive unknown inputs and faults in terms of projection-based detection methods.

Our final remark is dedicated to the following MMP,

$$\inf_{Q \in \mathcal{H}_\infty} \left\| \begin{bmatrix} -\hat{N}_1 & \hat{M}_1 \end{bmatrix} - Q \begin{bmatrix} -\hat{N}_2 & \hat{M}_2 \end{bmatrix} \right\|_\infty, \quad (145)$$

where  $\begin{bmatrix} -\hat{N}_i & \hat{M}_i \end{bmatrix}$  is the normalised SKR of system  $G_i = \hat{M}_i^{-1} \hat{N}_i, i = 1, 2$ , whose solution is defined as T-gap (Georgiou and Smith, 1990) and adopted in (Li and Ding, 2020a) under the concept of  $\mathcal{K}$ -gap for fault detection study. For our purpose, define

$$\mathcal{K}_{G_i}(\mathcal{H}_2^\perp) = \left\{ \begin{bmatrix} u \\ y \end{bmatrix} \in \mathcal{H}_2^\perp : \begin{bmatrix} -\hat{N}_i & \hat{M}_i \end{bmatrix} \begin{bmatrix} u \\ y \end{bmatrix} = 0 \right\} \in \mathcal{H}_2^\perp, i = 1, 2, \quad (146)$$

as a dual subspace to the  $\mathcal{H}_2$  image subspace  $\mathcal{I}_{G_i}$ . It turns out

$$\begin{aligned} \mathcal{P}_{\mathcal{K}_{G_i}(\mathcal{H}_2^\perp)} : \mathcal{H}_2^\perp &\rightarrow \mathcal{H}_2^\perp, \mathcal{P}_{\mathcal{K}_{G_i}(\mathcal{H}_2^\perp)} = \mathcal{I} - \mathcal{L}_{K_{G_i}^\sim} \mathcal{P}_{\mathcal{H}_2^\perp} \mathcal{L}_{K_{G_i}}, i = 1, 2, \\ \vec{\delta}(\mathcal{K}_{G_1}(\mathcal{H}_2^\perp), \mathcal{K}_{G_2}(\mathcal{H}_2^\perp)) &= \left\| \left( \mathcal{I} - \mathcal{P}_{\mathcal{K}_{G_1}(\mathcal{H}_2^\perp)} \right) \mathcal{P}_{\mathcal{K}_{G_2}(\mathcal{H}_2^\perp)} \right\|. \end{aligned}$$

Note that

$$\begin{aligned} \mathcal{I} - \mathcal{P}_{\mathcal{K}_{G_1}(\mathcal{H}_2^\perp)} &= \mathcal{L}_{K_{G_1}^\sim} \mathcal{P}_{\mathcal{H}_2^\perp} \mathcal{L}_{K_{G_1}} : \mathcal{H}_2^\perp \rightarrow \mathcal{H}_2^\perp, \\ \mathcal{P}_{\mathcal{K}_{G_2}(\mathcal{H}_2^\perp)} &= \mathcal{I} - \mathcal{L}_{K_{G_2}^\sim} \mathcal{P}_{\mathcal{H}_2^\perp} \mathcal{L}_{K_{G_2}} = \mathcal{L}_{I_{G_2}} \mathcal{L}_{I_{G_2}^\sim} + \mathcal{L}_{K_{G_2}^\sim} \mathcal{P}_{\mathcal{H}_2} \mathcal{L}_{K_{G_2}} : \mathcal{H}_2^\perp \rightarrow \mathcal{H}_2^\perp, \\ \implies \left( \mathcal{I} - \mathcal{P}_{\mathcal{K}_{G_1}(\mathcal{H}_2^\perp)} \right) \mathcal{P}_{\mathcal{K}_{G_2}(\mathcal{H}_2^\perp)} &= \mathcal{L}_{K_{G_1}^\sim} \begin{bmatrix} \mathcal{P}_{\mathcal{H}_2^\perp} \mathcal{L}_{K_{G_1}} \mathcal{L}_{I_{G_2}} \mathcal{P}_{\mathcal{H}_2^\perp} & \mathcal{P}_{\mathcal{H}_2^\perp} \mathcal{L}_{K_{G_1}} \mathcal{L}_{K_{G_2}^\sim} \mathcal{P}_{\mathcal{H}_2} \end{bmatrix} \begin{bmatrix} \mathcal{L}_{I_{G_2}^\sim} \\ \mathcal{L}_{K_{G_2}} \end{bmatrix}, \end{aligned}$$

which yields

$$\vec{\delta}(\mathcal{K}_{G_1}(\mathcal{H}_2^\perp), \mathcal{K}_{G_2}(\mathcal{H}_2^\perp)) = \left\| \begin{bmatrix} \mathcal{P}_{\mathcal{H}_2^\perp} \mathcal{L}_{K_{G_1}} \mathcal{L}_{I_{G_2}} \mathcal{P}_{\mathcal{H}_2^\perp} & \mathcal{P}_{\mathcal{H}_2^\perp} \mathcal{L}_{K_{G_1}} \mathcal{L}_{K_{G_2}^\sim} \mathcal{P}_{\mathcal{H}_2} \end{bmatrix} \right\|. \quad (147)$$

In (Georgiou and Smith, 1990), it has been proved that the operator norm on the right-hand side of (147) is equal to the solution of MMP (145), which implies

$$\vec{\delta}(\mathcal{K}_{G_1}(\mathcal{H}_2^\perp), \mathcal{K}_{G_2}(\mathcal{H}_2^\perp)) = \inf_{Q \in \mathcal{H}_\infty} \left\| \begin{bmatrix} -\hat{N}_1 & \hat{M}_1 \end{bmatrix} - Q \begin{bmatrix} -\hat{N}_2 & \hat{M}_2 \end{bmatrix} \right\|_\infty.$$

This result corrects the claim in (Li and Ding, 2020a) that MMP (145) is the gap from  $\mathcal{K}_{G_1}$  to  $\mathcal{K}_{G_2}$ .

## Appendix A: Proof of Lemma 1

By means of the plant model (76), control law (72)-(73) and the Bezout identity (74), we have

$$\begin{aligned}
& \begin{bmatrix} I & -K \\ -G & I \end{bmatrix}^{-1} \begin{bmatrix} I \\ 0 \end{bmatrix} = \begin{bmatrix} M & 0 \\ 0 & V_0 \end{bmatrix} \begin{bmatrix} M & -U_0 \\ -N & V_0 \end{bmatrix}^{-1} \begin{bmatrix} I \\ 0 \end{bmatrix} \\
& = \begin{bmatrix} M & 0 \\ 0 & -V_0 \end{bmatrix} \left( \begin{bmatrix} M_0 & U_0 \\ N_0 & V_0 \end{bmatrix} + \begin{bmatrix} \Delta_M \\ \Delta_N \end{bmatrix} \begin{bmatrix} I & 0 \end{bmatrix} \right)^{-1} \begin{bmatrix} I \\ 0 \end{bmatrix} \\
& = \begin{bmatrix} M & 0 \\ 0 & -V_0 \end{bmatrix} \begin{bmatrix} I + \Delta_1 & 0 \\ \Delta_2 & I \end{bmatrix}^{-1} \begin{bmatrix} \hat{V}_0 \\ -\hat{N}_0 \end{bmatrix} \\
& = \begin{bmatrix} M & 0 \\ 0 & -V_0 \end{bmatrix} \begin{bmatrix} (I + \Delta_1)^{-1} & 0 \\ -\Delta_2 (I + \Delta_1)^{-1} & I \end{bmatrix} \begin{bmatrix} \hat{V}_0 \\ -\hat{N}_0 \end{bmatrix}, \\
& \Delta_1 = \begin{bmatrix} \hat{V}_0 & -\hat{U}_0 \end{bmatrix} \begin{bmatrix} \Delta_M \\ \Delta_N \end{bmatrix}, \Delta_2 = \begin{bmatrix} -\hat{N}_0 & \hat{M}_0 \end{bmatrix} \begin{bmatrix} \Delta_M \\ \Delta_N \end{bmatrix}.
\end{aligned}$$

Since

$$V_0 \hat{N}_0 = N_0 \hat{V}_0, V_0 \hat{M}_0 = I + N_0 \hat{U}_0$$

leads to

$$\begin{aligned}
& V_0 \Delta_2 (I + \Delta_1)^{-1} \hat{V}_0 + V_0 \hat{N}_0 \\
& = N_0 (I - \Delta_1 (I + \Delta_1)^{-1}) \hat{V}_0 + \Delta_N (I + \Delta_1)^{-1} \hat{V}_0 = N (I + \Delta_1)^{-1} \hat{V}_0,
\end{aligned}$$

it turns out

$$\begin{aligned}
& \begin{bmatrix} M & 0 \\ 0 & -V_0 \end{bmatrix} \begin{bmatrix} (I + \Delta_1)^{-1} & 0 \\ -\Delta_2 (I + \Delta_1)^{-1} & I \end{bmatrix} \begin{bmatrix} \hat{V}_0 \\ -\hat{N}_0 \end{bmatrix} = \begin{bmatrix} M \\ N \end{bmatrix} (I + \Delta_1)^{-1} \hat{V}_0 \\
& \implies \begin{bmatrix} u \\ y \end{bmatrix} = \begin{bmatrix} I & -K \\ -G & I \end{bmatrix}^{-1} \begin{bmatrix} I \\ 0 \end{bmatrix} v = \begin{bmatrix} M \\ N \end{bmatrix} (I + \Delta_1)^{-1} \hat{v}.
\end{aligned}$$

Thus, the lemma is proved.

## References

- Beard, R.V. (1971). *Failure Accomodation in Linear Systems Through Self-Reorganization*. PhD Dissertation, MIT.
- Blanke, M., M. Kinnaert, J. Lunze and M. Staroswiecki (2006). *Diagnosis and Fault-Tolerant Control, 2nd Edition*. Springer. Berlin Heidelberg.
- Chen, J. and R. J. Patton (1999). *Robust Model-Based Fault Diagnosis for Dynamic Systems*. Kluwer Academic Publishers. Boston.
- Chiang, L. H., E. L. Russell and R. D. Braatz (2001). *Fault Detection and Diagnosis in Industrial Systems*. Springer. London.
- Ding, S. X. (2008). *Model-Based Fault Diagnosis Techniques - Design Schemes, Algorithms, and Tools*. Springer-Verlag.

- Ding, S. X. (2014a). *Data-Driven Design of Fault Diagnosis and Fault-Tolerant Control Systems*. Springer-Verlag. London.
- Ding, S. X. (2014b). Data-driven design of monitoring and diagnosis systems for dynamic processes: A review of subspace technique based schemes and some recent results. *Journal of Process Control* **24**, 431–449.
- Ding, S. X. (2020). *Advanced Methods for Fault Diagnosis and Fault-tolerant Control*. Springer-Verlag. Berlin.
- Ding, S. X., L. Li and M. Kruger (2019). Application of randomized algorithms to assessment and design of observer-based fault detection systems. *Automatica* **107**, 175–182.
- Ding, S. X., T. Jeinsch, P. M. Frank and E. L. Ding (2000). A unified approach to the optimization of fault detection systems. *International Journal of Adaptive Control and Signal Processing* **14**, 725–745.
- Ding, X., L. Guo and P. M. Frank (1993). A frequency domain approach to fault detection of uncertain dynamic systems. In: *Proc. of the 32nd Conference on Decision and Control*. Texas, USA. pp. 1722–1727.
- Ding, S. X., L. Li, D. Zhao, C. Louen and T. Liu (2022). Application of the unified control and detection framework to detecting stealthy integrity cyber-attacks on feedback control systems *Automatica* **142**, 110352.
- Feintuch, A. (1998). *Robust Control Theory in Hilbert Space*. Springer-Verlag. New York.
- Francis, B. A. (1987). *A Course in H-Infinity Control Theory*. Springer-Verlag. Berlin – New York.
- Frank, P. M. (1990). Fault diagnosis in dynamic systems using analytical and knowledge-based redundancy - a survey. *Automatica* **26**, 459–474.
- Frank, P. M. and X. Ding (1994). Frequency domain approach to optimally robust residual generation and evaluation for model-based fault diagnosis. *Automatica* **30**, 789–904.
- Frank, P. M. and X. Ding (1997). Survey of robust residual generation and evaluation methods in observer-based fault detection systems. *Journal of Process Control* **7(6)**, 403–424.
- Gao, Z. W., C. Cecati and S. X. Ding (2015). A survey of fault diagnosis and fault-tolerant techniques, part i: Fault diagnosis with model-based and signal-based approaches. *IEEE Trans. on Industrial Electronics* **62**, 3757–3767.
- Georgiou, T. T (1988). On the computation of the gap metric. *Syst. Contr. Letters* **11**, 253–257.
- Georgiou, T. T and M. C. Smith (1990). Optimal robustness in the gap metric. *IEEE Trans. on Automatic Control* **35**, 673–686.
- Gertler, J. J. (1998). *Fault Detection and Diagnosis in Engineering Systems*. Marcel Dekker. New York Basel Hong Kong.

- Hoffmann, J. W. (1996). Normalized coprime factorizations in continuous and discrete time – a joint state-space approach. *IMA Journal of Mathematical Control and Information* **13**(4), 359–384.
- Hou, M. and R. J. Patton (1996). An LMI approach to infinity fault detection observers. In: *Proceedings of the UKACC International Conference on Control*. pp. 305–310.
- Huang, B. and R. Kadali (2008). *Dynamic Modelling, Predictive Control and Performance Monitoring, a Data-Driven Subspace Approach*. Springer-Verlag. London.
- Hwang, I., S. Kim, Y. Kim and C.E. Seah (2010). A survey of fault detection, isolation, and reconfiguration methods. *IEEE Trans. Contr. Syst. Tech.* **18**, 636–653.
- Jolliffe, I.T. (1986). *Principal Component Analysis*. Springer-Verlag. New York, Berlin.
- Jones, H. (1973). *Failure Detection in Linear Systems*. PhD dissertation, MIT.
- Kato, T. (1995). *Perturbation Theory for Linear Operators*. Springer-Verlag. Berlin.
- Li, G., S. J. Qin and D. Zhou (2010). Geometric properties of partial least squares for process monitoring. *Automatica* **46**, 204–210.
- Li, L. and S. X. Ding (2020a). Gap metric techniques and their application to fault detection performance analysis and fault isolation schemes. *Automatica* **118**, 109029.
- Li, L. and S. X. Ding (2020b). Optimal detection schemes for multiplicative faults in uncertain systems with application to rolling mill processes. *IEEE Trans. on Control Systems Technology* **28**(6), 2432–2444.
- Mangoubi, R., M. Desai, A. Edelmayer and P. Sammak (2009). Robust detection and estimation in dynamic systems and statistical signal processing: Intersection, parallel paths and applications. *European Journal of Control* **15**, 348–369.
- Patton, R. J. and J. Chen (1993). Optimal unknown input distribution matrix selection in robust fault diagnosis. *Automatica* **29**, 837–841.
- Patton, R. J., P. M. Frank and R. N. Clark (Ed) (1989). *Fault Diagnosis in Dynamic Systems, Theory and Applications*. Prentice-Hall. Englewood Cliffs, NJ.
- Qin, S.J. (2003). Statistical process monitoring: Basics and beyond. *Journal of Chemometrics* **17**, 480–502.
- Venkatasubramanian, V., R. Rengaswamy, K. Yin and S.N. Kavuri (2003). A review of process fault detection and diagnosis part I: Quantitative model-based methods. *Computers and Chemical Engineering* **27**, 293–311.
- Vinnicombe, G. (2000). *Uncertainty and Feedback:  $H_\infty$  Loop-Shaping and the  $\nu$  Gap Metric*. World Scientific.
- Wang, J. L., G.-H. Yang and J. Liu (2007). An LMI approach to h-index and mixed  $h_-/h_{inf}$  fault detection observer design. *Automatica* **43**, 1656–1665.

- Zhong, M., S.X. Ding, J. Lam and H.B. Wang (2003). An LMI approach to design robust fault detection filter for uncertain LTI systems. *Automatica* **39**, 543–550.
- Zhong, M. Y., T. Xue and S.X. Ding (2018). A survey on model-based fault diagnosis for linear discrete time varying systems. *Neurocomputing* **306**, 51–60.
- Zhou, K. (1998). *Essential of Robust Control*. Prentice-Hall. Englewood Cliffs, NJ.